



Vrije Universiteit Brussel

Faculteit Geneeskunde en Farmacie
Vrije Universiteit Brussel
Laarbeeklaan 103
B-1090 Brussel

Nanobody-mediated imaging and inhibition of the immune checkpoint ligand PD-L1

Quentin Lecocq

Eindwerk, ingediend voor het behalen van de graad van Master in de Biomedische
Wetenschappen

Academiejaar 2015-2016

Promotor: Prof. Dr. Karine Breckpot
Co-promotors: Prof. Dr. Nick Devoogdt and Prof. Dr. Marleen Keyaerts
Begeleider: Katrijn Broos

Laboratorium voor Moleculaire en Cellulaire Therapie (LMCT)
Departement Basis (bio)-Medische Wetenschappen (BMWE)
Laarbeeklaan 103/E
B-1090 Brussel



CONFIDENTIALITY NOTICE

This document and the information in it are provided in confidence, for the sole purpose of “obtaining the degree of Master in Biomedical Sciences”, and may not be disclosed to any third party or used for any other purpose without the express written permission of Profs. Nick Devoogdt, Marleen Keyaerts and Karine Breckpot.

OUTLINE

List of abbreviations	5
Summary	6
Introduction	7
1. The function and dysfunction of the immune system in cancer	7
2. Inhibitory immune checkpoint regulation, a breakthrough in cancer immunotherapy	8
2.1. Background on inhibitory immune checkpoints	8
2.2. The PD-1/PD-L1 pathway	12
2.3. Cancer immunotherapy with PD-1/PD-L1 blockade	13
3. Tumor stratification, an essential aspect for treatment assignment	15
3.1. PD-1 and PD-L1 as biomarkers to predict responses to PD-1/PD-L1 blockade	15
3.2. Monoclonal antibodies as radiotracers to image PD-1 or PD-L1 in tumors	16
Research objectives	17
Material and methods	19
1. Mice	19
2. Cell lines, dendritic cells and T-cells	19
3. Production and characterization of lentiviral vectors	19
4. Transduction of cells with lentiviral vectors	19
5. Generation of nanobodies	19
6. Selection of nanobodies using surface plasmon resonance and flow cytometry ..	20
7. Large scale production, purification and quality control of nanobodies	20
8. Labeling of nanobodies using ^{99m}Tc	21
9. Pinhole SPECT/micro-CT imaging	21
10. Generation of single cell suspension from isolated tumors	22
11. Functional assays	22
11.1. Antigen presentation assay using dendritic cells	22
11.2. Antigen presentation assay using tumor cells	22
12. Flow cytometry	23
12.1. Surface staining	23
12.2. Analysis of nanobody binding to PD-L1	24
12.3. Intracellular staining	24
12.4. Cell viability assay	25
13. Statistical analysis	25

Results	26
1. <i>In vitro</i> characterization of anti-PD-L1 nanobodies	26
2. Imaging assays using anti-PD-L1 nanobodies	28
2.1. Labeling nanobody with ^{99m} Tc.....	28
2.2. Biodistribution studies.....	29
2.3. Nanobody accumulation in the tumor environment.....	31
3. <i>In vitro</i> functional assays using anti-PD-L1 nanobodies	35
3.1. Competition studies using Biacore instruments.....	35
3.2. Functional assay : Co-culture dendritic cells – CD8 ⁺ T-cells.....	35
3.3. Viability assay : Co-culture tumor cells – CD8 ⁺ T-cells.....	37
3.4. Functional assay : Co-culture tumor cells – CD8 ⁺ T-cells.....	38
Discussion	40
Acknowledgements	45
Bibliographical references	46

LIST OF ABBREVIATIONS

7-AAD: amino actinomycin-D Ab: antibody	Mreg: immature myeloid cells Nbs: nanobodies
AF700: alexa fluor	NK: natural killer
AMIDE: Medical Image Data Examiner APC: allophycocyanin	PD-1: programmed death-1 PD-L1: programmed death-ligand 1 PE: R-Phycoerythrin
BV421: brilliant violet	Percp Cy 5.5: Peridinin chlorophyll protein Cy 5.5 conjugate
CD: cluster of differentiation	PGE2: prostaglandin
CDR: complementary-determining regions	E2 RUs: response units
CTLA-4: cytotoxic T lymphocyte associated antigen 4	SDS-PAGE: dodecyl sulfate-polyacrylamide gel electrophoresis
CTLs: cytotoxic T lymphocytes	SHP2: Src homology 2 domain-containing tyrosine phosphatase 2
DCs: dendritic cells	SPECT: single photon emission computed tomography
DNA: deoxyribonucleotide EDC:1-(3-(dimethylamino)propyl)-3-ethylcarbodiimide	SPR: surface plasmon resonance
FasL: Fas ligand	TAMs: tumor-associated macrophages
FITC: fluorescein iso thio cyanate FR: framework regions	TB: Terrific Broth
HcAb: heavy chain antibody	TCR: T-cell receptor
ICMI: In Vivo Cellular and Molecular Imaging laboratory	TGF- β : transforming growth factor- β
IFN: interferon	TILs: tumor-infiltrating lymphocytes
IHC: immunohistochemistry	TIM3: T-cell immunoglobulin mucin protein 3
IL: interleukin	Tregs: regulatory T-cells
IMAC: immobilized metal affinity chromatography	VEGF: vascular endothelial growth factor
IPTG: isopropyl- β -D-thiogalactopyranoside	VHH: variable domain of the heavy chain antibody
iRs: inhibitory receptors	
Ka: association constant	
Kd: dissociation constant	
LAG3: lymphocyte activation gene 3 LAL: Limulus ameocyte lysate	
LB: Luria-Bertani	
LMCT: Laboratory of Molecular and Cellular Therapy	
mAbs: monoclonal antibodies	
M-CSF: macrophage colony-stimulating factor	
MDSCs: myeloid-derived suppressor cells MHC: major histocompatibility complex MMR: macrophage mannose receptor MOI: multiplicity of infection	

SUMMARY

Introduction: The immune system has the ability to specifically destroy tumor cells and to form an immunological memory to prevent cancer recurrence based on the expression of tumor antigens. This is evidenced by the fact that most tumors are infiltrated with CD8⁺ cytotoxic T lymphocytes (CTLs) that are generally referred to as tumor-infiltrating lymphocytes (TILs). Recently developed therapies aim to induce an antitumor immune response by providing the required stimuli to activate T-cells in an antigen specific way. However, once these active immune cells reach the tumor, they encounter strong inhibitory signals provided by the tumor and their supporting cells. Blocking these inhibitory mechanisms is an interesting approach to maintain and to reinforce the antitumor immune response. Therefore, we propose to target the inhibitory checkpoint ligand PD-L1 using nanobodies (Nbs) as these are stable, soluble, have a high affinity and specificity, and show an excellent tissue penetration, making them particularly suitable for tumor targeting.

Material and methods: After the production and characterization of Nbs against the inhibitory receptor ligand PD-L1, we selected three of them based on their affinity and specificity for recombinant PD-L1 protein and binding to both mouse and human PD-L1 expressing cells. We further evaluated whether purified PD-L1 specific Nbs can be used to visualize PD-L1 in the tumor environment. Therefore, radiolabeled Nbs were injected in tumor bearing mice and γ -decay was analyzed using SPECT/CT. Next, we performed a functional assay where PD-L1 expressing murine dendritic cells (DCs) or TC-1 tumor cells were co-cultured with murine CD8⁺ T-cells in presence or not of the selected anti-PD-L1 Nbs. The use of a blocking antibody (Ab) specific for PD-L1 served as a control. The principle is based on the knowledge that blocking interaction of inhibitory ligand/receptor couples during antigen presentation between DCs and antigen specific T-cells, can enhance T-cell functionality. We thereby measured the cytokine production by T-cells after 48 hours of co-culture using flow cytometry as this is representative for their functionality. Moreover, we also measured the effect of PD-L1 blockade on the viability of TC-1 tumor cells and T-cells in these co-cultures.

Results: The Nb characterization resulted in the selection of three Nbs specific for human mouse PD-L1. Imaging assays demonstrated that the accumulation of Nb C3 in the tumor environment correlates with the presence of PD-L1 on the tumor cells. Moreover, we showed that the functionality of mouse CD8⁺ T-cells co-cultured with DCs was significantly enhanced when using an anti-PD-L1 Ab or the Nb C7. Similarly, the presence of a blocking Ab during tumor cell-CD8⁺ T-cell interactions does significantly affect the functionality of CD8⁺ T-cells. However, PD-L1 blockade seemed not to affect the viability of tumor cells nor CD8⁺ T-cells.

Conclusion: Current findings suggest that Nbs, which specifically bind PD-L1 can be used for imaging purposes. Additionally, Nb-mediated blockade of the inhibitory receptor ligand PD-L1 resulted in enhanced functionality of T-cells co-cultured with DCs or TC-1 cells in an *in vitro* functional assay. These preliminary findings warrant further research into the use of Nbs as theranostics.

Signature Promotor:

Date:

INTRODUCTION

1. The function and dysfunction of the immune system in cancer

The immune system has the ability to specifically destroy tumor cells and to form an immunological memory to prevent cancer recurrence based on the expression of tumor antigens¹. This is evidenced by the fact that most tumors are infiltrated with CD8⁺ cytotoxic T lymphocytes (CTLs) that are generally referred to as tumor-infiltrating lymphocytes (TILs). These TILs when unhampered can kill tumor cells. This process was formerly known as cancer immunosurveillance and is the first phase, the so-called elimination phase, in the immunoediting that takes place as a consequence of bilateral communication between tumor cells and host immune cells as illustrated in Figure 1A².

Malignant progression is decided on during the equilibrium phase in which tumor cells that are resistant to TILs are selected for. It has become clear that surviving tumor cells have the ability to subvert normal immune regulation to their advantage. Tumor cells have developed mechanisms that interfere in every stage of the tumor specific immune response. An immune response starts with presentation of antigens by mature dendritic cells (DCs) to T-cells. In the tumor environment the DC function is inhibited by factors like transforming growth factor- β (TGF- β), interleukin (IL)-10, macrophage colony-stimulating factor (M-CSF), *et cetera*. Consequently, the differentiation from immature to mature DCs is blocked. Immature DCs express low levels of major histocompatibility complex (MHC) molecules, co-stimulatory molecules like CD80 (B7.1) or CD86 (B7.2), and pro-inflammatory cytokines like IL-12, while they express high levels of co-inhibitory molecules like programmed death-ligand 1 (PD-L1, B7-H1, CD274), and immunosuppressive cytokines like TGF- β and IL-10. Immature DCs are trapped in the tumor and induce anergy of effector T-cells, and expansion of regulatory T-cells (Tregs)³. Homing of effector T-cells from lymph nodes, the site where they are activated, to tumors is also impaired because tumor cells modulate the expression of T-cell attracting chemokines⁴. In addition, endothelial cells that form the tumor vasculature are able to block the extravasation and activity of effector T-cells⁴. Tumor cells further actively recruit and mold immunosuppressive cells like Tregs⁵ and immature myeloid cells (referred to as Mregs)⁶, including tumor-associated macrophages (TAMs)⁷ and myeloid-derived suppressor cells (MDSCs)⁸. To recruit and promote these cell populations, tumor cells secrete chemokines and factors like prostaglandin E2 (PGE2), vascular endothelial growth factor (VEGF), IL-10, and TGF- β . Together, Tregs and Mregs actively quench effector T-cells through inhibition of DC and T-cell activation. Mechanisms such as production of suppressive cytokines like IL-10 and TGF- β , production of reactive oxygen and nitrogen species, and triggering of inhibitory receptors like programmed death-1 (PD-1, CD279) are exploited for these purposes. Finally, tumors have developed direct mechanisms to prevail in the event that functional effector T-cells do reach the tumor. For instance, tumors can down-regulate MHC-I expression to avoid recognition by CTLs, express molecules like Fas ligand (FasL, CD95) and PD-L1 to induce T-cell death or anergy in case recognition would occur⁹. Once immunosuppressive cells and TIL resistant tumor clones take the overhand, TILs are rendered inactive and as such we enter the escape phase of the immunoediting process (Figure1B).

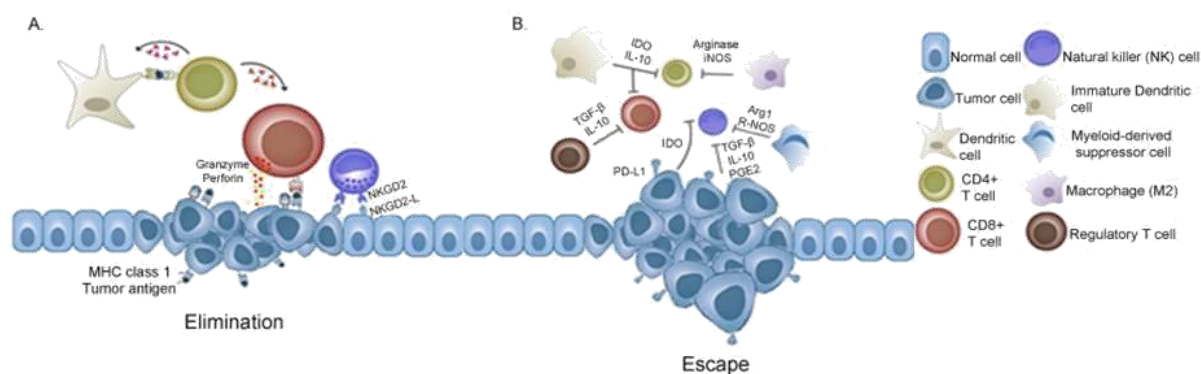


Figure 1: Immunoediting is a process that consists of three phases: *elimination, equilibrium and escape*.

(A) During the elimination phase, the immune system is able to recognize and eliminate tumor cells using natural killer (NK) cells, CD4⁺ and CD8⁺ T-cells. The equilibrium phase (not illustrated) is the phase during which tumor cells, with a non-immunogenic phenotype, can escape immune destruction and are selected for further growth.

(B) The selected tumor cells will breach the host immune defenses during the *escape phase* by gaining genetic and epigenetic changes. An example is the ability of tumor cells to secrete VEGF, which recruits tumor-associated immature myeloid cells inducing an immunosuppressive network, leading to tumor progression.

This knowledge has instigated research into the design of immunotherapy approaches to treat cancer. Much effort has been put in stimulation of *de novo* cancer specific CTLs, showing CTL induction in most patients¹⁰. However, the newly stimulated CTLs also encounter inhibitory mechanisms at the tumor environment. Therefore, methods to enhance and/or sustain their functionality in the tumor environment are receiving increasing attention. These methods include among others the use of monoclonal antibodies (mAbs) blocking inhibitory immune checkpoint pathways as well as methods to deplete or modulate suppressive immune cells at the tumor environment as reviewed elsewhere¹¹. Both CTL activating approaches as tumor environment modulating approaches have a substantial impact on the treatment of patients with advanced, previously untreatable malignancies, albeit often only in a subset of patients. It is expected that combinations of different cancer immunotherapy approaches will transform cancer treatment, improving the prognosis for many patients¹².

2. Inhibitory immune checkpoint modulation, a breakthrough in cancer immunotherapy

2.1. Background on inhibitory immune checkpoints

Three signals need to be provided by antigen-presenting cells, like DCs, to activate and differentiate naive T-cells (Figure 2)¹³. The first signal is provided by functional recognition of the peptide-MHC complex on the surface of DCs by the T-cell receptor (TCR) and its associated proteins, expressed on the surface of T-cells. The second signal, is provided by co-stimulatory surface molecules like CD80 and CD86, which are expressed on mature DCs and which bind to co-stimulatory receptors, in this case CD28, which is expressed on T-cells.

Such co-stimulatory ligand-receptor pairs are also referred to as stimulatory immune checkpoints. A third signal is provided by DCs under the form of cytokines and largely dictates the type of immune response that will be generated. For example, the production of interferon (IFN)- α/β or IL-12 as an answer to intracellular pathogens, promotes the differentiation of CD4⁺ T-cells into T helper 1 cells, which produce large amounts of IFN- γ and tumor necrosis factor- α (TNF- α), and which support the activation of CTLs¹⁴. Without the second and third signal, T-cells are unable to become activated, even when signal 1 is provided. Signal 1 and 2 can only be provided by DCs when they encountered pathogen or damage-associated molecular patterns, which bind pattern-recognition receptors and as such induce DC maturation.

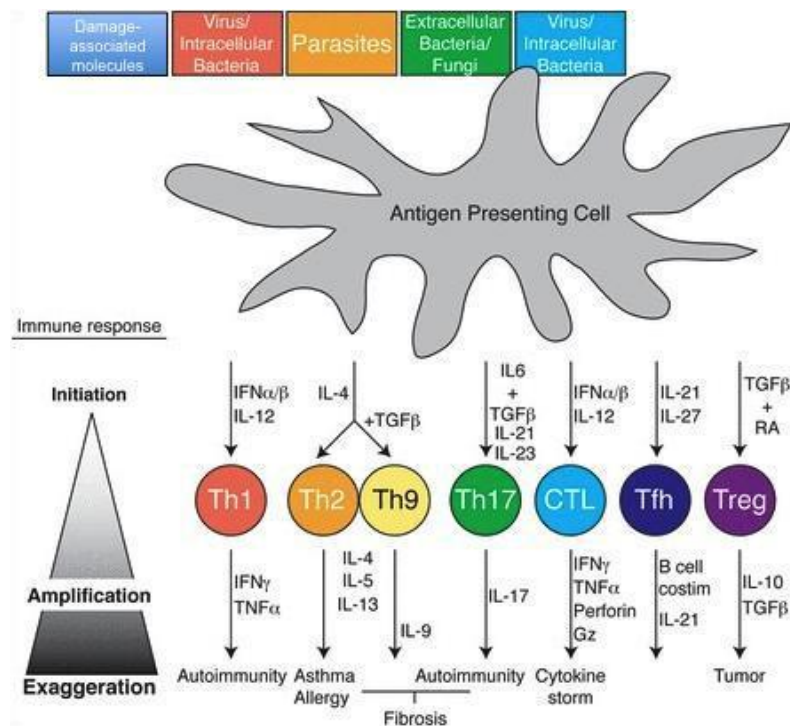


Figure 2: Activation and differentiation of T-cells. Antigen-presenting cells like DCs can recognize damage- or pathogen-associated molecular patterns through various pattern-recognition receptors. Consequently, DCs start a maturation process characterized by up-regulation of MHC and co-stimulatory molecules, and secretion of particular cytokines. The cytokine milieu dictates the differentiation of T-cells to a subset that is functionally specialized to respond to the encountered pathogen. Upon differentiation, T-cells also produce cytokines, as such providing feedback, amplifying and balancing the immune response to promote pathogen clearance. Sustained T-cell immune responses from any of the T-cell subsets results in a range of immunopathologies from autoimmunity to allergy and cancer. To avert exaggeration of the T-cell response, the immune system produces Tregs, a T-cell subset that puts the brake on a variety of inflammatory processes. Moreover, once activated, T-cells also express an array of inhibitory receptors (iRs), which also put a brake on the T-cell response¹⁴.

Activated T-cells will vigorously proliferate and differentiate into effector T-cells. Moreover, these cells can create a positive feedback loop by stimulating the expression of co-stimulatory proteins on antigen-presenting cells, hence amplifying the T-cell response¹⁴. Importantly, T-cell responses are tightly regulated. After containment of the hazardous event, for instance intruding pathogens, there are various processes brought in play to remove the still active immune cells. These so-called extrinsic and intrinsic inhibitory signals, provided to

active immune cells in the termination phase, are essential to circumvent collateral damage, unrestrained multiplication and even autoimmunity. Extrinsic inhibition is for example maintained by Tregs¹⁵. Involved in the intrinsic inhibition are inhibitory receptors (iRs) that are expressed on activated T-cells. Together with their ligands, iRs form inhibitory immune checkpoints. Figure 3 illustrates a number of different iRs expressed on T-cells.

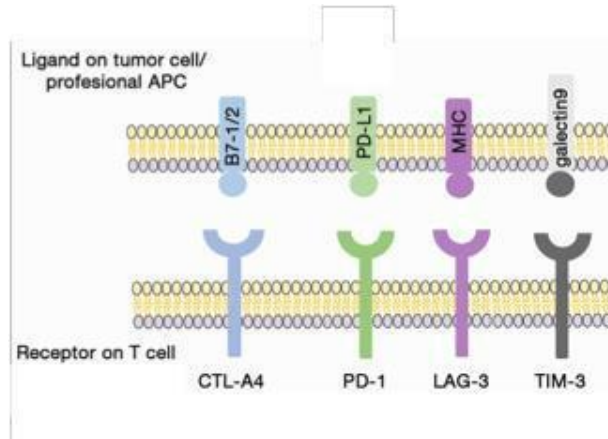


Figure 3: iRs implicated in the control of T-cell responses. Activated T-cells express iRs that together with their ligand form inhibitory immune checkpoints. Their expression is instigated to prevent sustained activation of T-cells. The iRs shown in figure 3 are cytotoxic T-lymphocyte antigen-4 (CTLA-4), PD-1, T-cell immunoglobulin domain and mucin domain-3 (TIM3) and lymphocyte-activation gene 3 (LAG3)¹⁶.

The best-studied iRs in the context of cancer immunology are CTLA-4 (CD152) and PD-1, which bind to CD80 (B7.1)/CD86 (B7.2) and PD-L1 (B7-H1)/PD-L2 (B7-DC) respectively. Other receptors, involved in inhibition of the T-cell function during cancer development include LAG3 (CD223) and TIM3 (CD336). As this thesis focuses on the inhibitory signals mediated by the interaction between PD-L1 and PD-1, we will only briefly summarize how triggering of CTLA-4, TIM3 or LAG3 affects antitumor immunity, while in the following section we will provide a detailed description of the PD-1/PD-L1 pathway.

CTLA-4, a homologue of the co-stimulatory molecule CD28 is expressed on CD4⁺ and CD8⁺ T-cells after activation while Tregs express it constitutively. This iR shows a high affinity for CD80 and CD86 present on DCs leading to the inhibition of T-cell proliferation, cell cycle progression, and IL-2 synthesis¹⁷. In contrast, interaction of CTLA-4 on Tregs to its ligands is believed to enhance Treg activity¹⁸.

LAG3 is an activation-induced cell surface protein expressed by T-cells, B cells, NK cells, Tregs and plasmacytoid DCs. This CD4-like molecule down-regulates the proliferation and activity of effector T-cells without hampering their viability¹⁹. Importantly LAG3 on Tregs, as well as on CD8⁺ T-cells was shown to endow them with suppressive activity²⁰. The binding partner of LAG3 is MHC-II, for which the expression is generally linked to antigen-presenting cells like DCs. Binding of LAG3 to MHC-II on DCs inhibits their maturation and as such T-cell activation²¹. Importantly, MHC-II expression is not restricted to antigen-presenting cells, also Tregs and melanoma cells can express MHC-II²². These cells exploit this MHC-II expression to interact with LAG3 on effector T-cells. Tregs, which acquire MHC-II via trochocytosis, exploit MHC-II to suppress LAG3 expressing CTLs, while melanoma cells exploit this MHC-II expression to protect themselves against LAG3 expressing CTLs.

TIM3 is expressed on active CD4⁺ and CD8⁺ T-cells and interacts with galectin-9. This will trigger the termination of immune responses and can even lead to T-cell death. Moreover, TIM3 is a negative regulator of antitumor immune responses as it causes T-cell exhaustion and stimulation of MDSCs²³.

Receptor	Ligand(s)	Modulation	Proposed mode of action
CTLA-4 (CD152)	CD80 (B7.1) CD86 (B7.2)	Ipilimumab (Yervoy [®]), fully human anti-CTLA-4 mAb, Bristol-Myers Squibb) → FDA and EMA approved. Tremelimumab (fully human anti-CTLA-4 mAb, Pfizer, MedImmune) → FDA approved.	Blockade of negative signals to CTLA-4 positive effector T-cells. Blockade of Treg activity and even depletion of CTLA-4 expressing Treg through antibody-dependent T-cellular cytotoxicity (ADCC).
PD-1 (CD279)	PD-L1 (CD274, B7-H1), PD-L2 (CD273, B7-DC)	Nivolumab (Opdivo [®]), fully human anti-PD-1 mAb, Bristol-Myers Squibb) → FDA and EMA approved. Pembrolizumab (Keytruda, humanized anti-PD-1 mAb, Merck) → FDA and EMA approved. MEDI0680 (APM-514, MedImmune) Pidilizumab (CT-011, humanized anti-PD-1 mAb, CurTech)	Blockade of negative feedback provided to PD-1 expressing effector T-cells. Depletion of PD-1 expressing Treg through ADCC.
TIM3 (CD336)	Gal9 (Galeitin 9)	Anti-human TIM3 mAbs → in development (Tesarö).	Blockade of TIM3 enhances effector T-cell functionality. Blockade of TIM3 affects Treg functionality. Blockade of TIM3 enhances the ability of tumor-infiltrating DCs to sense danger.
LAG3 (CD223)	MHC-II	Recombinant soluble LAG3-Ig fusion protein (IMP321) → in development (Prima Biomed). Anti-LAG3 mAbs (IMP701, Novartis and BMS-986016, Bristol-Myers Squibb) → in development.	IMP321 acts as an immune adjuvant. anti-LAG3 mAbs enhance effector T-cell functionality.

Table 1: Overview of strategies that are studied to interfere with inhibitory immune checkpoint pathways^{24, 25}.

A crucial aspect of the immunosuppressive tumor environment is the ability of tumors to skew the balance between co-stimulation and co-inhibition towards co-inhibition, thus dampening antitumor immune responses. This is effective against both spontaneous and *de novo* induced antitumor immunity. Several strategies are being developed to neutralize the effect of iRs as their ligands are co-opted by tumors to dampen antitumor immunity. So far, much effort has been put in developing mAbs or soluble antigens as a tool to bind and hamper the signaling of these iRs. A summary of these so-called immune checkpoint modulators and their proposed mode of action is provided in Table 1.

It is fair to state that the early results obtained in melanoma patients using mAbs such as ipilimumab (anti-CTLA-4) and nivolumab (anti-PD-1) have reinvigorated the field of cancer immunotherapy, and have changed the way cancer is treated today^{26, 27}. Unleashing the immune system to fight cancer has become an option for the treatment of various cancers including lung, breast, bladder and renal cancers. As the list of iRs is growing, the number of mAbs under development is growing and blocking of some of these iRs, such as LAG3 and TIM3, is being pursued in the clinic. The increasing clinical use of mAbs that block iRs has revealed two main challenges: the challenge to predict which iR or combination thereof should be targeted in a patient and the challenge to combine this iR modulation with other therapies in patients that have tumors, which are poorly infiltrated with effector T-cells²⁸.

2.2. The PD-1/PD-L1 pathway

Programmed death-1 receptor (PD-1) is a member of the B7 receptor family. It was originally identified as a gene that is highly expressed by cells undergoing programmed cell death, hence its name²⁹. PD-1 is up-regulated upon activation of T-cells, although it has been shown on human T-cells that PD-1 can be up-regulated in the absence of TCR triggering through the addition of cytokines³⁰. Although PD-1 as an iR is mainly associated with T-cells, its expression is not limited to activated T-cells. PD-1 is also expressed on activated B cells and myeloid cells^{31,32}. Moreover high levels of PD-1 are present intracellularly in Tregs. These are ready to be shuttled to the cell surface upon TCR stimulation³³.

The ligands for PD-1 are B7-H1 (PD-L1) and B7-DC (PD-L2). Expression of PD-L1 can be induced on different T-cell types, including monocytes, DCs, mast cells, T and B cells, epithelial, endothelial and muscle cells. In contrast, the expression of PD-L2 is restricted to DCs, macrophages and mast cells^{34,35,36}. It is also important to note that PD-L1 expression has been reported on several human and mouse tumors³⁷. Similar to PD-1, PD-L1 can bind to multiple surface markers. Besides its interaction with PD-1, it has been described that PD-L1 can bind CD80 (B7.1). The interaction of PD-L1 with both PD-1 and CD80 reflects the complexity of the signaling pathways that involve PD-L1^{38,39}.

It was shown that CD80 expressed on T-cells delivers an inhibitory signal to T-cells following its ligation with PD-L1 *in vitro*^{38,40}. Conversely, PD-L1 expressed on T-cells transduced an inhibitory signal to T-cells after its interaction with CD80³⁸. So far, it has not been demonstrated that similar T-cell-T-cell interactions occur *in vivo*. Moreover, it remains to be clarified whether interaction of CD80 expressed on DCs and MDSCs, with B7-H1 on T-cells would result in a similar inhibitory signal, although some studies allude to this situation⁴¹. Binding of PD-L1 to PD-1 is generally accepted to have an inhibitory outcome (Figure 4), although contradictory results have been obtained *in vitro* showing both negative and positive signaling of PD-L1 on T-cell proliferation and cytokine production⁴². Despite these contradicting *in vitro* studies, stimulation of PD-1 by PD-L1 has been linked to several immune repressing events *in vivo*, such as conversion of naive CD4⁺ T-cells to Treg⁴³ and enhanced proliferation of Treg⁴⁴. Moreover, stimulation of PD-1 on effector T-cells hampers their cell functionality among others by inhibition of kinases involved in T-cell activation³², induction of cell death²⁹ and modulation of the duration of T-cell-DC or T-cell-T-cell contact by down-regulation of the TCR^{45,46,47}. The net effect of this all is a reduced number of T-cells, which in addition show a reduced capacity to secrete cytokines^{48,49}. Tumor cells also use the PD-1/PD-L1 pathway to evade antitumor immunity. Many human cancers aberrantly express PD-L1, which is linked to so-called intrinsic and adaptive immune resistance. Intrinsic resistance refers to the expression of PD-L1 caused by genetic alterations and activation of several signaling pathways. Although not yet fully understood, recent studies link PD-L1 expression on cancer cells to over expression of MYC⁵⁰ and BRCA2⁵¹ mutations. Adaptive resistance refers to the up-regulation of PD-L1 on tumor cells as a consequence of an inflammatory environment⁵². Indeed, activated CD4⁺ T helper 1 cells, CD8⁺ T-cells and NK cells produce high amounts of IFN- γ , and as such induce up-regulation of PD-L1.

Cancer cells that express PD-L1 are protected from cell death as PD-L1 provides anti-apoptotic stimuli⁵³ and as they become refractory to CTL mediated killing^{54,55}. Moreover, interaction between PD-L1 expressed on tumor cells and PD-1 expressed on effector T-cells directly induces T-cell apoptosis⁵⁶. Therefore, it is not surprising that expression of PD-L1 is a poor prognostic factor in several cancer types, including ovarian cancer^{57,58}, renal cancer⁵⁹, pancreatic cancer⁶⁰, hepatocellular cancer⁶¹ and breast cancer^{62,63}.

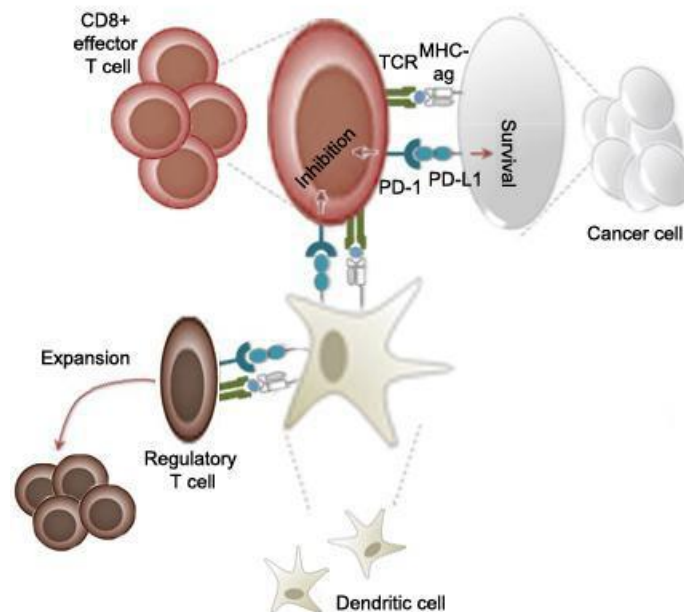


Figure 4: The PD-1/PD-L1 interaction between DCs and T-cells, DCs and Tregs, and finally between tumor cells and T-cells. The net effect after interaction of T-cells with DCs is the inhibition of effector T-cells and the stimulation of Tregs. Additionally, interaction between effector T-cells and cancer cells via the PD-1/PD-L1 pathway will lead to the inhibition of these effector T-cells hence protecting the cancer cells from being destroyed.

2.3. Cancer immunotherapy with PD-1/PD-L1 blockade

Different mAbs that disrupt the PD-1/PD-L1 axis are evaluated in a clinical setting. These can be categorized into mAbs that target PD-1 or PD-L1. Promising PD-1 targeting mAbs include nivolumab (Bristol-Myers Squibb); pembrolizumab (Merck) and pidilizumab (CureTech), while promising PD-L1 targeting mAbs include MPDL3280A (Genentech) and BMS-936559 (Bristol-Myers Squibb) (Table 2).

Anti-PD-1 mAbs have shown highly durable response rates with acceptable toxicity in large phase I studies for treatment of patients with melanoma, non small cell lung cancer, renal cell carcinoma and other solid tumors^{27, 64}. As a consequence anti-PD-1 mAbs have been tested in phase III clinical trials, mainly for the treatment of melanoma patients. In some of these studies, patients already received prior treatment like treatment with ipilimumab (anti-CTLA-4 mAbs). Despite the failure of ipilimumab and the advanced stage of the disease, treatment with nivolumab or pembrolizumab resulted in impressive survival results, albeit with occasional reports of high-grade treatment-related adverse events^{65, 66}. Consequently, both PD-1 targeting mAbs were FDA approved. Also pidilizumab, which has been mainly evaluated for treatment of patients with hematologic malignancies has delivered on its promise⁶⁷.

Target	Drug information	Clinical response rate	Phase	Patients
PD-1	Nivolumab Humanized IgG4a Bristol-Myers Squibb	12.8% in treatment-refractory metastatic melanoma, castrate-resistant prostate cancer, RCC, NSCLC, or CRC	1	39
		28% in advanced melanoma, 18% in NSCLC, 27% in RCC	1	296
		40% in melanoma treated with nivolumab + ipilimumab, 20% in nivolumab followed by ipilimumab	1	86
		87% in relapsed or refractory Hodgkin's lymphoma	1	23
		14.5% in refractory NSCLC	2	117
		31.7% in advanced melanoma progressed after anti-CTLA-4	3	405
		40% in previously untreated melanoma without BRAF mutation	3	418
		17% in previously treated advanced NSCLC	2	129
		29% in previously treated advanced RCC	2	34
		20% in advanced squamous-cell NSCLC	3	272
		57.6% (nivolumab+ipilimumab), 19% (ipilimumab), 43.7% (nivolumab) in stage III/IV melanoma	3	945
PD-1	Pembrolizumab Humanized IgG4k Merck	38% in melanoma	1	135
		26% in ipilimumab-refractory advanced melanoma	1	173
		63% versus 0% in stage IV NSCLC patients with high and low nonsynonymous mutation burden	1	29
		19.4% in advanced NSCLC	1	495
		40% and 0% in mismatch repair-deficient/proficient CRC	2	41
		33% (pembrolizumab) and 11.9% (ipilimumab) in advanced melanoma	3	834
PD-1	Pidilizumab Humanized IgG1 CureTech	51% in diffuse large B cell lymphoma (after HSCT)	2	66
		66% in relapsed follicular lymphoma	2	32
PD-L1	MPDL3280A Fc-modified human IgG1b Genentech/Roche	21% in advanced incurable cancer NSCLC, SCLC, melanoma, RCC, CRC, gastric cancer, head and neck squamous cell carcinoma, breast cancer, ovarian, pancreatic cancer, uterine cancer, sarcoma, pancreaticoduodenal cancer	1	277
		52% in metastatic bladder cancer	1	68
PD-L1	BMS-936559 Fully human IgG4a Bristol-Myers Squibb	17.3% in melanoma, 11.7% in RCC, 10.2% in NSCLC, 5.9% in ovarian cancer	1	207

Table 2: Clinical trials using mAbs that block the PD-1/PD-L1 axis (adapted from⁶⁸).

Targeting PD-L1 has been studied as a second option to interrupt negative signaling towards T-cells. This approach could potentially be more interesting as PD-L1 provides negative signals to T-cells by interacting with PD-1 as well as CD80. PD-L1 targeting mAbs would prevent both of these interactions, while PD-1 targeting mAbs would only prevent the PD-1 mediated negative signaling. On the other hand targeting of PD-1 prevents its interaction with PD-L2, and as such abrogates PD-L2/PD-1 mediated negative signaling to T-cells, while potentially allowing PD-L2 to interact with a second receptor to convey co-stimulatory signals^{36, 69}. Thus different biological effects can be expected when using anti-PD-1 or anti-PD-L1 targeting mAbs.

Anti-PD-L1 mAbs, including BMS-956559 and MPDL3280A have been evaluated in phase I clinical trials in a variety of indications like bladder cancer, head and neck cancer and gastrointestinal malignancies^{65, 70}. While BMS-956559 is no longer under clinical development⁷¹, other anti-PD-L1 mAbs like MPDL3280A (Roche)⁷², MEDI4736 (MedImmune/AstraZeneca)⁷³ and MSB0010718C (EMD Serono)⁷⁴ have been successfully developed and tested in phase I clinical trials. Further development of these mAbs is ongoing.

Although different biological effects were expected when using PD-1 or PD-L1 targeting mAbs, it seems that both achieve comparable levels of clinical response. Also treatment-related toxicities are comparable for both anti-PD-1 and anti-PD-L1 treatments. One mild side effect, i.e. fatigue, is frequently observed. More severe side effects include inflammatory pneumonitis or interstitial nephritis, however, reports on these immune-related adverse events are not as frequent as reports on severe adverse events when using anti-CTLA-4 mAbs⁶⁸. Nonetheless, the treatment related adverse events caution us that blockade of inhibitory immune checkpoints should preferentially be performed locally, i.e. at the tumor environment.

3. Tumor stratification, an essential aspect for treatment assignment

3.1. PD-1 and PD-L1 as biomarkers to predict responses to PD-1/PD-L1 blockade

Treatment with antagonistic mAbs to block the PD-1 signaling axis has shown encouraging results across different indications. Nonetheless, a substantial number of patients does not respond well. Because of this and as mAb therapy comes at a considerable cost, there is a need to accurately predict which patients will benefit from this treatment. A number of correlative studies utilizing invasive biopsy in conjunction with immunohistochemistry (IHC) suggest that PD-1 expression on TILs could serve as a predictive marker⁷⁵. Similarly, it has been investigated whether PD-L1 expression in the tumor environment can serve as a biomarker. Indeed, across multiple cancer types, there is a strong positive correlation between pre-treatment PD-L1 expression (irrespective of its expression on tumor cells or infiltrating immune cells) and therapeutic response to PD-1/PD-L1 pathway inhibition^{52, 72}. Nonetheless, patients showing PD-1 or PD-L1 expression can fail anti-PD-1 or anti-PD-L1 mAb therapy⁷⁶, while patients that show no PD-L1 expression were reported to benefit from anti-PD-L1 mAb therapy^{54, 77}. This can be explained by the high heterogeneity of tumors.

Both the expression of PD-1 and PD-L1 are highly heterogeneous within both the primary tumor and distant metastases. Moreover, the expression of PD-1 and PD-L1 are likely to change in time. Consequently, a static picture of a biopsy is not ideal to predict the therapy outcome. Moreover, the IHC technique has the additional limitations that it does not provide information about the PD-1/PD-L1 expression in metastatic lesions, and that it can only be performed on tumors that are accessible for biopsy. Therefore, there is a compelling need to develop a non-invasive imaging strategy to determine the presence of immune checkpoints in cancer patients before as well as during the course of their treatment.

3.2. Monoclonal antibodies as radiotracers to image PD-1 or PD-L1 in tumors

Monoclonal Abs specific for PD-L1 and PD-1 have been studied for imaging purposes. Herein, the mAbs are radiolabeled and SPECT/CT imaging is performed to visualize accumulation of the mAbs at the tumor region. So far, imaging of PD-L1 expression has been performed in syngeneic and xenograft animal models using an engineered PD-1 derived fragment, or a mouse anti-human, a hamster anti-mouse (Figure 5) and more recently a fully humanized anti-PD-L1 mAb^{76, 78, 79}. These studies show the feasibility of non-invasive PD-L1 imaging *in vivo*. Similarly, the expression of mouse PD-1 using a radiolabeled hamster anti-mouse mAb was recently shown⁸⁰.

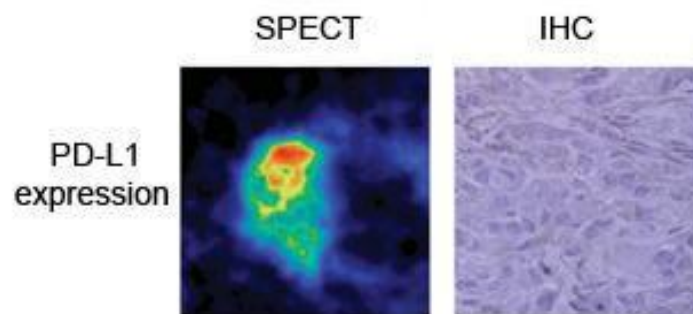


Figure 5: Here, the PD-L1 expression on breast cancer xenograft SK-Br-3 is analyzed using SPECT scan with radiolabeled Abs (left) or IHC (right)⁷⁸. Note that analyzing PD-L1 using SPECT provides more information about the dispersed expression of it. The color code going from green (low expression of PD-L1) towards red (high expression of PD-L1) is more descriptive than the brown dots, seen with IHC. Moreover, IHC will not detect much PD-L1 expression thus considering the patient as non responder to anti-PD-L1 therapy, when by chance a biopsy is taken in the „green“ zone of the tumor .

RESEARCH OBJECTIVES

Immune checkpoint blockade has emerged as a new paradigm in cancer immunotherapy. Although there is cause for optimism, there are still several aspects that merit further attention in order to bring immune checkpoint blockade into the standard of care cancer therapies.

1. There is a growing list of receptor-ligand couples that can potentially be exploited in cancer therapy²⁵, which brings forth the challenge to determine which immune checkpoint pathways dominate in a particular tumor, as this is critical to choose the best-suited inhibitor or combinations thereof.
2. Systemic administration of high doses of mAbs entails the risk of immune-related adverse events due to off-target events. It was shown in a mouse model of colon cancer that peritumoral delivery of anti-CTLA-4 mAbs at low doses results in tumor rejection with minimal toxicity⁸¹. However mAbs have low tissue penetrating capacities⁸². Therefore, it remains to be determined whether mAbs can be delivered at therapeutic doses without side effects.
3. The use of mAbs for therapy purposes is associated with a high cost (e.g. the cost of a short-course, 4-dose Ipilimumab or Pembrolizumab regimen is about €90.000⁸³).

Thus there is a need to develop novel tools for imaging and to design an effective therapy.

We propose to generate nanobodies (Nbs) against immune checkpoint molecules. Nbs, also called single-domain variable fragments of heavy chain-only antibodies have a prolate shape of approximately 2.5 nm in diameter and 4.2 nm in length, and a 12-15 kDa size (Figure 6). They are stable, soluble and have a high specificity and affinity⁸⁴. Furthermore, Nbs efficiently enter tissues where they rapidly and specifically bind their antigens. Unbound Nbs are rapidly cleared through renal elimination. These traits make them ideal candidates for tumor targeting⁸⁴.

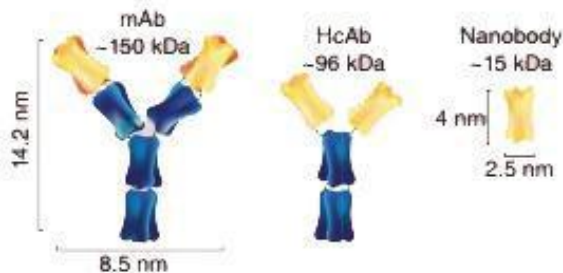


Figure 6: Schematic overview of different antibody formats. From left to right; the conventional Ab, the heavy chain only Ab (HcAb) obtained from Camelidae and finally the variable domain of the heavy chain (VHH) or Nb.

In this thesis, we hypothesize that Nbs specific for inhibitory immune checkpoint molecules could be used as a diagnostic for detection of dominant immune checkpoint pathways in the tumor (= tumor stratification), and that delivery of Nbs to the tumor could block immune checkpoint signaling (= cancer therapy).

Rationale for using Nbs for tumor stratification and therapy: The ICMI lab has extensively studied Nbs for imaging of cancer markers like HER2^{85, 86}, epithelial growth factor receptor⁸⁷, carcinoembryonic antigen⁸⁸ and paraprotein in breast, lung, colon cancer and multiple myeloma respectively. These endeavors have resulted in a first in-human clinical trial at the UZ Brussel to evaluate the safety of radio-labeled anti-HER2 Nbs for PET-imaging in healthy volunteers and breast cancer patients⁸⁵. Moreover, Nbs were used to visualize macrophage mannose receptor (MMR) expressing tumor-associated macrophages (TAMs) within the tumor nest⁸⁹, which proves that Nbs are a sensitive tool that can be used to visualize markers present on cancer-associated immune cells. In addition, the LMCT recently showed that Nbs specific for MMR can be used to bind TAM resembling *in vitro* generated macrophages as well as macrophages *in vivo* (unpublished data). These findings, suggest that delivery of Nbs that block immune checkpoint pathways in the tumor is feasible.

In this thesis we focus on Nbs specific for PD-L1 to deliver a proof-of-concept on the use of Nbs for tumor stratification and therapy, hence as theranostics. We chose for PD-L1 because:

1. PD-L1 is highly expressed in the tumor environment both on tumor cells as a variety of tumor-infiltrating immune cells.
2. PD-L1 provides negative signals to effector T-cells by interacting with PD-1 as well as CD80. Antagonistic Nbs that bind PD-L1 could prevent both of these interactions and as such tackle two inhibitory signaling pathways.
3. PD-L1 has shown promise as a biomarker, predictive for the therapy response to anti-PD-1 and anti-PD-L1 therapy.

The specific objectives of this thesis can be summarized as follows:

1. To fully characterize the library of PD-L1 specific Nbs that is available at ICMI, and select Nbs that show high affinity for human or mouse PD-L1.
2. To evaluate whether purified PD-L1 specific Nbs can be used to visualize PD-L1 in the tumor environment (TC-1 mouse model).
3. To evaluate whether the selected high affinity PD-L1 specific Nbs have the ability to block binding of PD-L1 to PD-1 and if so, whether this blockade during antigen presentation by mouse DCs or TC-1 tumor cells enhances the viability and functionality of effector T-cells.

When successful, Nb-mediated tumor stratification would facilitate the decision-making on whether a patient is eligible for PD-L1 targeted treatment. Moreover, Nbs could be used to follow up the expression of PD-L1 in the tumor microenvironment during the treatment with Nbs that block immune checkpoint signaling. As such we can adjust the treatment regimen according to the PD-L1 expression in the patients' tumor.

MATERIALS & METHODS

1. Mice

Female 6-12 weeks old C57BL/6 and OT-I mice were purchased from Charles River. OT-I mice carry a transgenic CD8⁺ TCR specific for the MHC-I restricted ovalbumin (OVA) peptide SIINFEKL. Mice deficient in PD-L1 expression (PD-L1^{-/-}) were a kind gift from Adrian Liston (KUL). Animals were handled according to the institutional guidelines. Experiments were approved by the Ethical Committee for use of laboratory animals of the VUB.

2. Cell lines, dendritic cells and T-cells

TC Wu (Johns Hopkins University, Baltimore, MD) kindly provided the mouse lung epithelial cell line TC-1, which were cultured in RPMI medium, consisting of Roswell Park Memorial Institute 1640 medium (Sigma-Aldrich) supplemented with 10% FCI serum (Harlan), 2 mmol/L L-glutamine (L-Glu; Sigma-Aldrich), 100 U/mL penicillin, 100 µg/mL streptomycin (PS; Sigma-Aldrich), 1 mmol/L sodium pyruvate and non-essential amino acids (Sigma-Aldrich).

Human embryonal kidney (HEK) 293T-cells were purchased from the American Type Culture Collection (ATCC) and were cultured in DMEM medium, consisting of Dulbecco's modified Eagle's medium (Sigma-Aldrich) supplemented with 10% FBS (Harlan), L-Glu and PS. Mouse bone marrow-derived DCs were generated as described in Breckpot et al⁹⁰.

Mouse CD8⁺ OT-I cells were obtained from the spleen of OT-I mice. To that end, spleens were isolated and reduced to single cell suspensions, after which CD8⁺ cells were selected using magnetically activated cell sorting with CD8α⁺ T-cell Isolation Kit (MiltenyiBiotec).

3. Production and characterization of lentiviral vectors

The packaging plasmid pCMVΔR8.9 and the VSV.G encoding plasmid pMD.G were a gift from D. Trono (University of Geneva). The transfer plasmid encoding PD-L1, pHR⁺-huPD-L1, was previously described⁴⁹. The plasmid pHR⁺-mPD-1, which encodes mouse PD-1, was generated as described for pHR⁺-huPD-L1⁴⁹. Similarly, the plasmid pHR⁺-mPD-L1, which encodes mouse PD-L1, was generated as described for pHR⁺-huPD-L1⁴⁹. The transfer plasmid encoding short hairpin RNA against mouse PD-L1 was kindly provided by Dr. David Escors (Pamplona, Spain)⁹¹. The mouse CD274 sgRNA CRISPR/Cas9 All-in-One lentiviral transfer vector was purchased from Applied Biological Materials Inc. The production of lentiviral vectors and their characterization by flow cytometry was performed as described⁹².

4. Transduction of cells with lentiviral vectors

Transduction of HEK293T and TC-1 cells was carried out at a multiplicity of infection (MOI) of 10, using the protocol previously described to transduce human DCs⁹⁰.

5. Generation of nanobodies

The generation of Nbs specific for human and/or mouse PD-L1 was outsourced to the Nanobody Service Facility of the VIB. Briefly, alpaca's (*Vicugna pacos*) were immunized 6 times at a weekly interval using 100 µg recombinant human PD-L1-Fc, alternated with recombinant mouse PD-L1-Fc (R&D system, 156-B7 and 1019-B7 respectively).

Subsequently, peripheral blood lymphocyte mRNA was converted to cDNA, from which Nb-coding sequences were amplified and ligated in the pHEN4 phagemid vector. Using M13K07 helper phages, the Nb library was expressed on phages. Specific Nb-phages were enriched by several rounds of selection on microtiter plates (Nunc) coated with recombinant human or mouse PD-L1-Fc. Individual colonies were screened in ELISA for antigen recognition, after which specific binders were sequenced. Forty-two Nbs specific for human and/or mouse PD-L1 were isolated from three different immune Nb phage-display libraries.

6. Selection of nanobodies using surface Plasmon resonance and flow cytometry

To further select potentially interesting Nbs, E.coli WK6 cells were transformed with Nb-coding pHEN4 plasmids and cultured in 10 mL Luria-Bertani broth (LB) containing 100 µg/mL Ampicillin (Fermentas) for 6 hours at 37°C. Nb-expression was induced over night with 1 mM isopropyl-β-D-thiogalactopyranoside (IPTG) while shaking at 200 rpm and 28°C. Subsequently, cultures were centrifuged for 10 minutes at 1643xg and 4°C, after which the bacterial pellet was frozen at -80°C. One day later, 2 mL phosphate buffered saline (PBS, Sigma-Aldrich) was added to the thawed bacterial pellets and pellets were stirred for 30 minutes at 4°C. Periplasmic proteins extracted by osmotic shock, were collected by centrifugation for 20 minutes at 730xg and 4°C, followed by 0.22 µm filtration (Millipore). These periplasmic proteins were used for analysis via surface Plasmon resonance (SPR) on the Biacore2000 device. To that end, mPD-L1His or huPD-L1His (Sino Biological Inc., 50010-M08H and 10084-H08H) were immobilized on a CM5 sensor chip. This sensor chip was pre-treated for 7 minutes with 400 nM 1-(3-(dimethylamino)propyl)-3-ethylcarbodiimide (EDC) and 100 mM N-hydroxy-succinimide (NHS). The mPD-L1His and huPD-L1His were diluted in 10 mM sodium acetate (pH 5.0) and injected to reach response units (RUs) of 701.3 and 882.0 respectively. Next, the free ester surface was blocked by injection of 1 M ethanolamine-HCl. All samples, including samples containing mPD-1 or huPD-1 (R&D Systems), were run at a flow rate of 10 µL per minute. In another channel (e.g. Fc1) an identical procedure was followed but without the ligand. This channel was used as a reference to calculate background response units (RUs). Each ligand-analyte interaction was expressed as a relative RUs, defined as RU (Fc2)-RU(Fc1). The periplasmic extracts were further used in flow cytometry to evaluate their binding to human and/or mouse PD-L1 expressed on HEK293T-cells.

7. Large scale production, purification and quality control of nanobodies

Genes of selected Nbs, were recloned into the vector pHEN6 to encode a C-terminal His₆ tag. Also Nb BCII10 and R3B23, specific for β-lactamase and 5T2 multiple myeloma cells respectively, were produced as these are used throughout the study as negative controls. The plasmid constructs were transformed into E. coli WK6 cells and stored as glycerol stocks. Glycerol stocks were thawed and inoculated on LB/ampicillin agar plates to obtain single colonies. Single colonies were picked and cultured overnight at 37°C in a 50 mL falcon tube containing 15 mL LB medium. At an optic density of 0.6-0.9 at 600 nm, bacteria were transferred to shaker flasks containing 2 L Terrific Broth (TB) supplemented with 0.1%

glucose and ampicillin. These were grown until an optic density of 0.6 to 0.9 was reached. Nb expression was then induced with 1 mM IPTG for 16 hours at 28 °C. After pelleting the cells, the periplasmic proteins were extracted by osmotic shock as described above. Nanobodies were purified from periplasmic extracts using immobilized metal affinity chromatography (IMAC) followed by size exclusion chromatography (SEC). The extracts were admixed with His-select resin (2 mL per extract obtained from 2 L cultures) and shaken for 1 hour at 200 rpm and room temperature. This mixture was loaded on a PD10 column and allowed to empty by gravitational flow. Collected beads were washed with 20-50 mL PBS and the bound Nb was eluted with 10 mL 0.5 M imidazole. Eluted fractions were collected and Nb concentrations were determined using in NanoDrop. The AKTA Explorer, equipped with a SuperdexHiload 75 µg 16/600column was used for further SEC purification. Fractions containing Nbs, obtained after IMAC were centrifuged to clear aggregates and contaminants. Buffers were freshly prepared, filtered, and degassed prior to running the column. During the run at 2 mL per minute, absorbance at 280 nm and conductivity were monitored. The Nbs were eluted approximately after 100 mL was run. The fractions containing Nbs were pooled and the Nb concentration was measured by NanoDrop. Protein purity was assayed by 12% sodium dodecyl sulfate-polyacrylamide gel electrophoresis (SDS-PAGE) under reducing condition followed by staining with Coomassie Blue. Purified Nbs were run at different concentrations over immobilized mouse and human PD-L1 on a CM5 chip. The RUs representing Nb/PD-L1 interactions were recorded in real-time to give a sensorgram, allowing calculation of the association (K_a) and dissociation rate constant (K_d) using the Biacore2000 software. Finally, endotoxins were measured in the LAL (Limulus amoebocyte lysate) assay. The latter was performed as recommended by the manufacturer (Pierce™ LAL Chromogenic Endotoxin Quantification Kit, Thermofisher).

8. Labeling of nanobodies with ^{99m}Tc

^{99m}Tc was used to label the His₆ tail of the Nbs. [$^{99m}\text{Tc}(\text{H}_2\text{O})_3(\text{CO})_3$]⁺ was synthesized by adding 1 mL of eluate (0.74-3.7 GBq) from a $^{99\text{Mo}}\text{-}^{99m}\text{Tc}$ generator (Drytec: GE Healthcare) to an Isolink kit (Mallinckrodt Medical BV). This mix was boiled for 20 minutes. After neutralization with 1 M HCl, the [$^{99m}\text{Tc}(\text{H}_2\text{O})_3(\text{CO})_3$]⁺ was added to the 1 mg/mL Nb solution and incubated for 90 minutes at 52°C. The ^{99m}Tc -Nb solution was purified on a NAP-5 column (GE Healthcare) pre-equilibrated with PBS to remove unbound [$^{99m}\text{Tc}(\text{H}_2\text{O})_3(\text{CO})_3$]⁺ and finally filtered through a 0.22 µm filter (Millipore) to remove aggregates. The labeling efficiency was determined both directly after labeling and after purifications by instant thin-layer chromatography with 100% acetone as the mobile phase.

9. Pinhole SPECT/micro-CT Imaging

Mice were anesthetized 10-15 minutes prior to imaging with a mixture consisting of 18.75 mg/kg ketamine hydrochloride (Ketamine 1000; CEVA) and 0.5 mg/kg medetomidine hydrochloride (Domitor; Pfizer). Micro-CT imaging was followed by pinhole SPECT on separate systems. Micro-CT was performed using a dual-source CT scanner (Skyscan 1178; Skyscan) with 60 kV and 615 mA at a resolution of 83 µm. The total body scan time was 2

minutes. Images were reconstructed using filtered back projection (NRecon; Skyscan). Subsequently, total body pinhole SPECT was performed once at 60 minutes after injection of ^{99m}Tc labeled Nbs using a dual-head γ -camera (e.cam180; Siemens Medical Solutions), mounted with 2 multipinhole collimators (three 1.5 mm pinholes in each collimator, 200 mm focal length, and 80 mm radius of rotation). Images were acquired over 360° in 64 projections of 10 seconds into 128x128 matrices, resulting in a total imaging time of 14 minutes per animal. The SPECT images were reconstructed using an iterative reconstruction algorithm (ordered-subset expectation maximization) modified for the 3-pinhole geometry and automatically reoriented for fusion with CT images based on six ^{57}Co landmarks. Images were further analyzed using AMIDE (Medical Image Data Examiner software). After imaging, mice were sacrificed and all organs (including tumors when applicable) were isolated to measure radioactivity using a gamma counter.

10. Generation of single cell suspensions from isolated tumors

Mice were killed by neck dislocation after which tumors were excised. Single cell suspensions were prepared from these tumors using the GentleMACS single cell isolation protocol (Miltenyi Biotec).

11. Functional assays

We performed several *in vitro* functional assays to analyze whether Nbs are antagonists.

11.1. Antigen-presentation assay using dendritic cells

Mouse DCs were pulsed for 1 hour with 5 $\mu\text{g}/\text{mL}$ of the peptide SIINFEKL (R&D Systems). Pulsing was performed in RPMI1640 medium in the absence of supplements. Thereafter, 2×10^4 peptide-pulsed DCs resuspended in 50 μL RPMI medium were plated per well in a 96 well plate. Subsequently, we added 50 μL RPMI medium containing 10 μg anti-PD-L1 mAbs (BioXCell, 10F.9G2), isotype matched control mAbs (BioXCell, LTF2), the selected Nbs or a control Nbs (R3B23 or BCII10). After this step, we sorted CD8^+ OT-I spleen cells and added 2×10^5 T-cells to each well (in 100 μL RPMI medium). In addition, we plated 2×10^5 T-cells in 200 μL RPMI medium, which we did not stimulate as well as 2×10^5 T-cells in 200 μL RPMI medium containing a 1/200 dilution of anti-CD3/anti-CD28 Ab coated beads. Each condition was set up in triplicate. One day after the start of the co-culture, the supernatant was replaced with 200 μL RPMI medium containing a protein transport inhibitor (BD Golgi plug/stopTM). Sixteen hours later, the cells were analyzed in flow cytometry for the production of IFN- γ and TNF- α .

11.2. Antigen-presentation assay using tumor cells

Similar to the co-cultures described above, we set up co-cultures using tumor cells as antigen-presenting cells. Briefly, CD8^+ OT-I spleen cells were co-cultured with SIINFEKL-pulsed PD-L1 positive TC-1 or PD-L1 negative TC-1 cells, either in the presence or absence of mAbs and Nbs. We evaluated (i) the viability of the tumor cells and OT-I cells, and (ii) the activation of the OT-I cells (production of IFN- γ and TNF- α) in flow cytometry.

12. Flow cytometry

12.1. Surface staining

Cells were washed twice with FACS buffer, i.e. PBS containing 1% bovine serum albumin (Sigma-Aldrich) and 0.1% NaN₃ (Sigma-Aldrich). Next, the cells were incubated for 30 minutes at 4 °C with the required Abs diluted in FACS buffer to the desired concentration. The surplus of Abs was removed using an excess FACS buffer and centrifugation at 3000 rpm for 3 minutes in the petalfuge. Cells were acquired on the LSRFortessa and analyzed with FACSDiva (Becton Dickinson) or Flow Jo (Treestar inc.) software. The tables below show the Ab panels used throughout the different experiments.

Panel used for analysis of human or mouse PD-L1 expression on lentivirally modified HEK293T and TC-1 cells.			
Marker	Fluorochrome	Clone	Manufacturer
huPD-L1	APC	29E.2A3	Biolegend
moPD-L1	APC	10F.9G2	Biolegend

Panel used to analyze expression of PD-1 and PD-L1 on single cell suspensions of isolated tumors			
Marker	Fluorochrome	Clone	Manufacturer
CD45	V450	30-F11	BioLegend
CD4	AF 700	RM4-5	BD
CD8	APC-H7	53-6.7	BD
PD-L1	APC	10F.9G2	BioLegend
PD-1	PE	RMP1-30	BioLegend

Panel used to analyze expression of PD-1, PD-L1 and CD80 on OT-I cells or DC destined for <i>in vitro</i> functional assays			
OT-I T-cells			
Marker	Fluorochrome	Clone	Manufacturer
CD3	Percp Cy5.5	154-2C11	BD
CD8	FITC	53-6.7	BD
PD-1	PE	RMP1-30	BioLegend
PD-L1	APC	10F.9G2	BioLegend
CD80	BV421	16-10A1	BD

DCs			
Marker	Fluorochrome	Clone	Manufacturer
CD11c	APC	HL3	BD
CD80	BV421	16-10A1	BD
PD-L1	PE	10F.9G2	BioLegend

12.2. Analysis of nanobody binding to PD-L1

In order to evaluate binding of the purified PD-L1 Nbs we performed flow cytometry on human and mouse PD-L1 expressing HEK293T-cells. The His-tagged Nbs that bind to the PD-L1 protein on the surface of the cells can be detected by adding a commercially available anti-histidin Ab, which in turn can be detected using a PE labeled anti-mouse IgG Ab.

Panel used to analyze binding of Nbs to human or mouse PD-L1 expressing HEK293T-cells.			
Marker	Fluorochrome	Clone	Manufacturer
Anti-His	/	AD1.1.10	ABDSerotec
Anti-mouse IgG	PE	A51	BD

12.3. Intracellular staining

Mouse OT-I T-cells co-cultured for 48 hours with SIINFEKL pulsed DCs or TC-1 cells were first stained with Abs specific for CD3 and CD8 as described in 12.1. After the surface staining, the intracellular staining for IFN- γ and TNF- α was performed according to the manufacturer's instructions (BD biosciences). Living cells were discriminated from dead cells by performing a Zombie Yellow™ staining.

Panel used to analyze the production of IFN- γ and TNF- α by OT-I cells co-cultured with antigen presenting cells during the <i>in vitro</i> functional assay			
Marker	Fluorochrome	Clone	Manufacturer
Zombie Yellow™	BV605	/	BioLegend
CD3	Percp Cy5.5	154-2C11	BD
CD8	APC-H7	53-6.7	BD
TNF- α	FITC	MP6-XT22	BD
IFN- γ	PeCy7	XMG 1.2	BioLegend

12.4. Cell viability analysis

To analyze the viability of OT-I cells and TC-1 cells that were co-cultured, cells were first stained with an anti-CD45 Ab to discriminate OT-I cells (CD45⁺) from TC-1 cells (CD45⁻). Subsequently, the cells were incubated with Annexin-V and 7-aminoactinomycin D (7-AAD).

Panel used to analyze the viability of OT-I and TC-1 cells after their co-culture in the <i>in vitro</i> functional assay			
Marker	Fluorochrome	Clone	Manufacturer
CD45	BV605	30-F11	BioLegend
Annexin-V	PE	/	BD
DNA	7-AAD	/	BD

13. Statistical analysis

Where appropriate, a one-way ANOVA was performed with post-hoc Bonferroni correction. Differences were considered significant at $p < 0.05$. Statistical significance is indicated in the figures as * ($p < 0.05$), ** ($p < 0.01$) or *** ($p < 0.001$).

RESULTS

1. *In vitro* characterization of anti-PD-L1 nanobodies reveals C3, C7, E4 as potential cross-reactive nanobodies.

Forty-two anti-PD-L1 Nbs, belonging to 13 sequence families and coming from three different libraries, were available for evaluation. For these 42 Nbs, crude periplasmic extracts were generated and used as a source of Nbs for (i) ELISA screening (recognition of immobilized recombinant mouse and/or human PD-L1); (ii) affinity measurements on immobilized mouse and human PD-L1 antigens using SPR on the Biacore2000 instrument and (iii) flow cytometry to measure their binding on mouse and/or human PD-L1 expressed on cells. The results of these assays are summarized in table 3.

Name	Code	ELISA (OD-value)			Biacore (affinity)		Flow cytometry (MFI)			
		Mouse	Human	No Ag	Mouse	Human	Human		Mouse	
							PD-L1+	PD-L1-	PD-L1+	PD-L1-
R2LL26	A1	2.5794	0.0945	0.0968	no	23 nM	10174	699	116	129
R2L125	B1	0.897	0.2141	0.195	123nM	6nM	716	688	-56	-45
R2LL51	C1	3.6802	0.4291	0.1554	327pM	143nM	14251	1254	1101	215
R2LL82	C2	3.743	0.4727	0.1838	ND	ND	ND	ND	ND	ND
R2LL67	C3	3.7828	1.3394	0.1525	140pM	32nM	3315	272	431	36
R2LL2	C4	3.7723	0.8755	0.1812	187pM	342nM	10792	348	581	43
R2LL68	C5	3.6962	0.8694	0.1243	ND	ND	ND	ND	ND	ND
R2LL12	C6	3.7024	0.6344	0.1532	289 pM	94nM	7528	691	770	208
R2LL50	C7	3.7739	1.1077	0.3419	3.1nM	27nM	25555	2300	275	-4
R2LL83	C8	3.7573	1.1562	0.1777	ND	ND	ND	ND	ND	ND
R2LL37	C9	3.6941	0.7949	0.1238	2.2 nM	44nM	5050	515	461	234
R2LL28	C10	3.7161	0.6557	0.2129	6.7nM	141nM	20856	572	452	98
R2LL35	C11	3.8662	0.5572	0.2175	12nM	246nM	27267	577	378	105
R2LL33	C12	3.5804	0.4049	0.0917	11.4nM	181nM	19746	1116	348	-46
R2LL46	C13	3.5369	1.0144	0.1249	33nM	162nM	26347	2671	36	-8
R2LL18	C14	3.6701	0.7512	0.0911	1.8nM	71nM	8650	1350	96	91
R2LL20	C15	3.6368	0.4461	0.1504	6.5nM	335nM	13530	684	27	-51
R2LL34	C16	3.6768	0.5203	0.1853	15nM	520nM	15277	411	202	142
R2LL66	D1	3.6391	2.8148	2.4878	12nM	291 nM	3054	506	196	-72
R2L166	E1	3.6391	2.8148	2.4878	2.3 nM	12nM	4944	681	135	-29
R2L97	E2	2.9933	1.0964	0.5687	5.6 nM	94nM	1301	34	283	119
R2L113	E3	3.9717	3.0705	1.7095	ND	ND	1893	429	-46	-62
R2L164	E4	3.9304	3.0665	1.0478	ND	ND	5110	259	69	64
R2L37	E5	2.8355	0.1141	0.0989	14 nM	54nM	1704	454	37	-7
R2L155	E6	2.4418	0.6909	0.3211	6.9 nM	217nM	2348	500	-54	-20
R2LL10	F1	3.6697	0.4092	0.2388	ND	ND	ND	ND	ND	ND
R2L14	G1	3.5102	0.3395	0.1831	4.4 nM	50nM	2795	616	120	-5
R2L54	G2	4	2.3125	1.4331	5.5 nM	158nM	1936	423	341	43
R2L60	G3	3.7986	1.6653	0.77	5.0 nM	907nM	1543	699	55	-46
R2L62	G4	3.892	1.3798	0.7293	6.2nM	74nM	822	305	227	88
R2L270	G5	3.9486	3.5717	2.5806	3.9nM	16nM	3357	336	289	-29
R2L10	G6	4	3.7483	2.912	5.0nM	21nM	5902	8522	-47	21
R2L106	G7	1.0341	0.3335	0.2443	3.4nM	129nM	2870	159	319	141
R2LL23	H1	3.7375	0.8713	0.6773	ND	ND	ND	ND	ND	ND
R2LL40	I1	3.5587	0.2076	0.2332	67nM	322nM	3697	2309	28	-35
CD274cl6	J1	ND	ND	ND	0	271nM	1426	480	-55	-63
CD274cl3	K1	ND	ND	ND	no	5.7nM	24201	284	158	-86
CD274cl4	K2	ND	ND	ND	no	3.9nM	19997	383	-37	-72
CD274cl17	K3	ND	ND	ND	no	3.5nM	21607	374	-56	-94
ThamM1	L1	2.307	ND	0.899	15nM	34nM	ND	ND	ND	ND
ThamH1	M1	ND	5.975	0.254	13nM	17nM	ND	ND	ND	ND

Table 3: Summary of the *in vitro* results using periplasmic extracts containing anti-PD-L1 Nbs (n = 1).

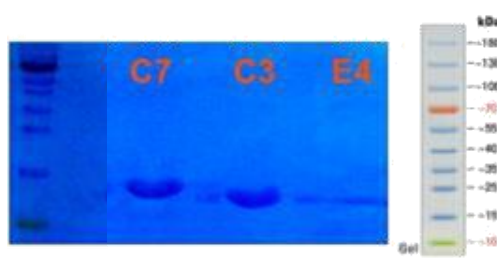


Figure 8: Representative reducing SDS-PAGE for the four purified Nbs. For each Nb, 5 µg was loaded. The result shows a single band corresponding to the typical size of a Nb (n = 1).

We already performed kinetic Biacore analyses using crude periplasmic extracts with estimated Nb concentrations (Table 3). These analyses were repeated with the purified Nbs, confirming that Nb C3, C7 and E4, show a high affinity for the mouse PD-L1 protein, while their affinity for human PD-L1 is lower (Table 4). Moreover, the purified Nbs were used in flow cytometry (1 µg/sample), confirming binding to human PD-L1 (C3, C7, E4) and mouse PD-L1 (C3, C7, E4) expressed on lentivirally modified HEK293T-cells (Figure 9).

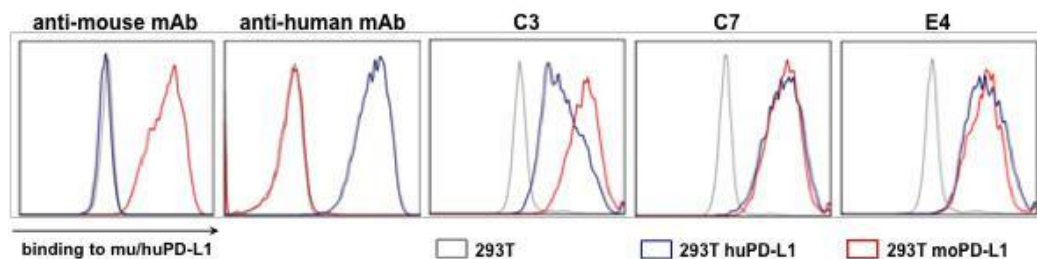


Figure 9: Representative flow cytometry results, showing staining of non-modified HEK293T-cells (grey line), or HEK293T-cells lentivirally modified to express mouse PD-L1 (moPD-L1, red line) or human PD-L1 (huPD-L1, blue line) with mAbs specific for mouse or human PD-L1, or Nb C3, C7, E4 (n = 3).

In the remainder of the project Nbs C3, C7 and E4 were further evaluated for their applicability for imaging and therapy purposes.

2. Imaging assays suggest that Nbs, which specifically bind mouse PD-L1 can be used for imaging purposes

2.1. Nbs C3, C7 and E4 can be efficiently labeled with ^{99m}Tc

To study the applicability of Nbs C3, C7 and E4 for SPECT/CT imaging, we first evaluated whether the Nbs can be efficiently labeled with ^{99m}Tc , a radioactive label that is detectable by the gamma camera. The labeling was performed using standard protocols and is based on the complexation of ^{99m}Tc -tricarbonyl with the hexahistidine-tag present within the Nbs. Non-complexed ^{99m}Tc was removed by gel filtration and possible aggregates present within the eluted ^{99m}Tc -Nb preparation were removed by filtration. The radiochemical purity was assessed by iTLC measurements. The radiochemical purity should be >98% to ensure at least 1 mCi injection into mice. This was the case for all three selected Nbs (Figure 10).

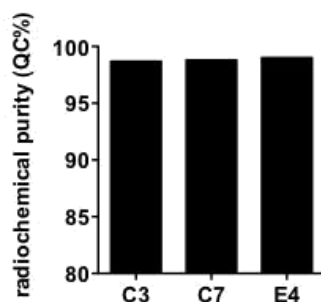


Figure 10: Radiochemical purity of the selected Nbs specifically recognizing mouse PD-L1 (n ≥ 1).

2.2. Biodistribution analyses of Nbs C3, C7 and E4 in wild type versus PD-L1^{-/-} mice show specificity and a different distribution pattern

To address the biodistribution and specificity of the Nbs C3, C7 and E4 in vivo, we injected wild type C57BL/6 mice and PD-L1^{-/-} mice intravenously with 10 µg of the labeled Nbs (1 mCi). SPECT/CT scanning was performed one hour later on anesthetized mice. The images were reconstructed and visualized using AMIDE software. Eighty minutes after the SPECT/CT scan, mice were euthanized, organs isolated, weighed, and accumulated radioactivity was measured in a gamma counter.

The results of the SPECT/CT scanning showed that signals are detected in the kidneys and bladder of both wild type and PD-L1^{-/-} mice. This is explained by the fact that Nbs are excreted in the urine. Besides signals in kidneys and bladder, Nbs C3, C7 and E4, gave relatively high signals in organs out of the renal system in wild type mice (Figure 11).

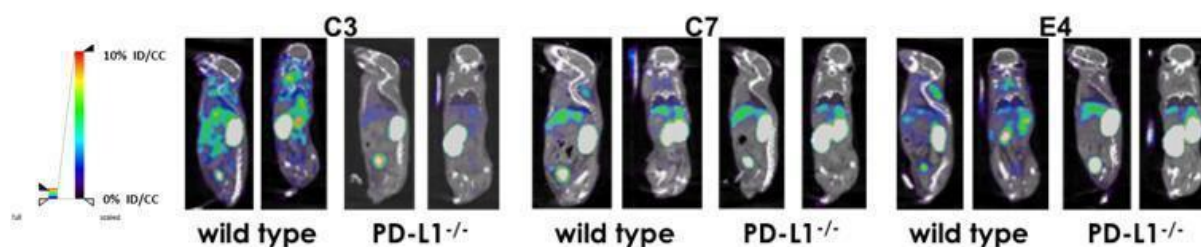


Figure 11: Results of SPECT/CT scans to determine the biodistribution of ^{99m}Tc-Nb C3, C7 or E4 injected in wild type (left) or PD-L1^{-/-} (right) C57BL/6 mice (n = 1, number of mice per condition = 3).

To determine the anatomical location of these signals, we performed gamma counting on isolated organs. Nbs C3 showed relative high radioactivity in thymus, heart, lungs, liver, spleen, intestines, lymph nodes and brown adipose tissue of wild type mice as well as in the liver of PD-L1^{-/-} mice (Figure 12). A similar anatomical distribution was observed for Nb E4 (Figure 13), albeit with lower signals as for Nb C3. In contrast, Nb C7 predominantly gave high signals in the liver and spleen of both wild type and PD-L1^{-/-} mice (Figure 14).

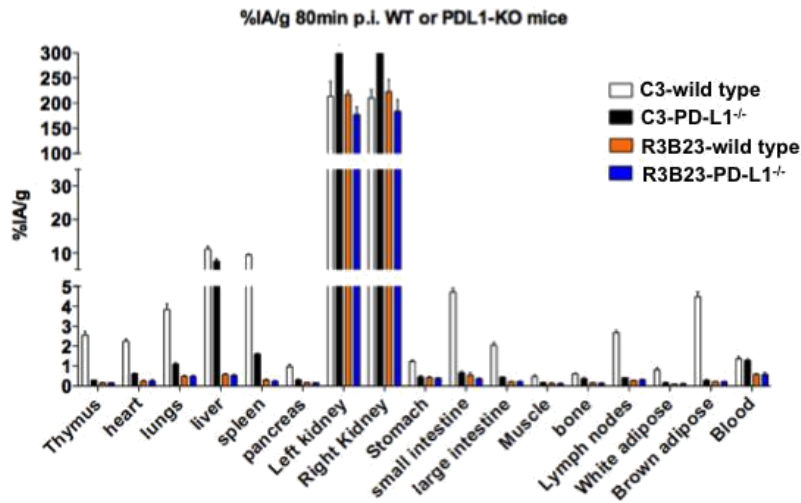


Figure 12: Gamma counting of isolated organs from C57BL/6 wild type and PD-L1^{-/-} mice injected with ^{99m}Tc-Nb C3 (n = 1, number of mice per condition = 3).

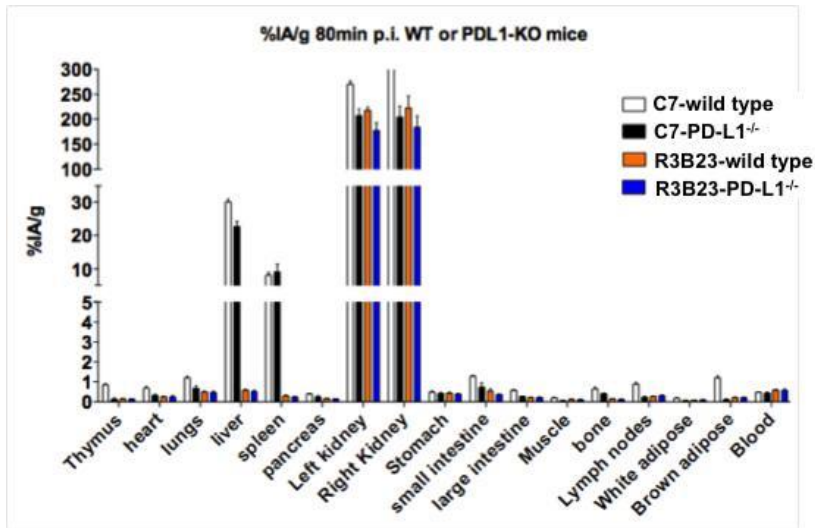


Figure 13: Gamma counting of isolated organs from C57BL/6 wild type and PD-L1^{-/-} mice injected with ^{99m}Tc-Nb C7 (n = 1, number of mice per condition = 3).

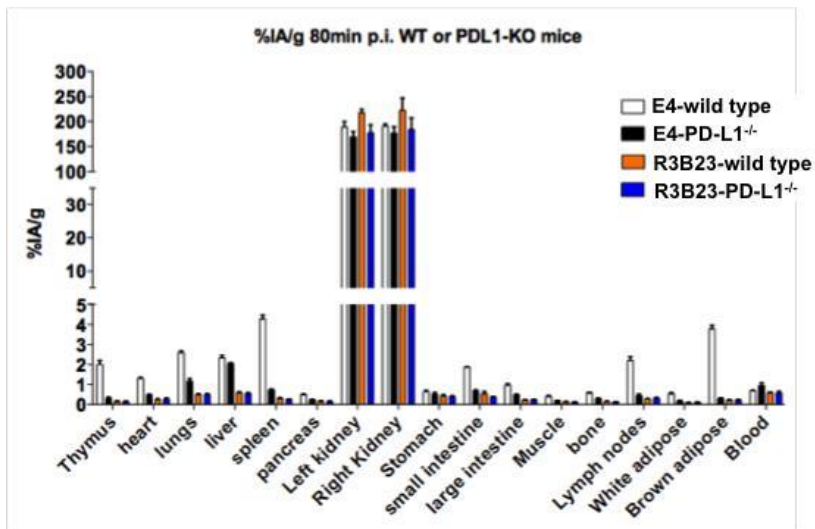


Figure 14: Gamma counting of isolated organs from C57BL/6 wild type and PD-L1^{-/-} mice injected with ^{99m}Tc-Nb E4 (n = 1, number of mice per condition = 3).

2.3. Nb C3 accumulates in the tumor environment

Since Nb C3 gave the predicted biodistribution and highest radioactive signals in C57BL/6 wild type mice, we next addressed whether this Nb can be used for visualization of PD-L1 expressed on tumor cells or tumor-infiltrating immune cells. Therefore, we first generated a PD-L1 deficient mouse tumor cell line. Hereto, we transduced TC-1 lung epithelial cells that express the oncogene E7 of HPV, with lentiviral vectors that harbor a short hairpin RNA targeting mouse PD-L1. This cell line was referred to as TC-1-shPD-L1. In addition, we generated a TC-1 cell line that was highly positive for PD-L1 by modification with lentiviral vectors encoding mouse PD-L1. This cell line was referred to as TC-1-mPD-L1. Expression of PD-L1 on wild type TC-1 cells, TC-1-shPD-L1 and TC-1-mPD-L1 cells was evaluated by flow cytometry (Figure 15).

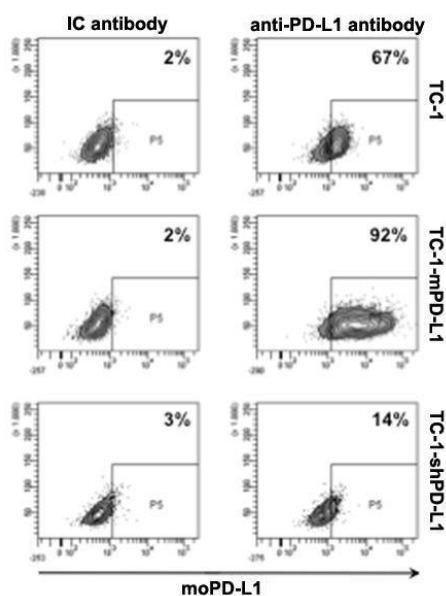


Figure 15: Expression of PD-L1 on TC-1, TC-1-mPD-L1, TC-1-shPD-L1 was evaluated in flow cytometry. The flow cytometry graphs are representative for 5 independent experiments (n = 5). The left panel shows the cells stained with isotype matched control (IC) Abs. The right panel shows the cells stained with anti-PD-L1 Abs.

Subsequently, the TC-1, TC-1-mPD-L1 and TC-1-shPD-L1 cells were transplanted subcutaneously in C57BL/6 wild type mice. Tumor growth was followed up every other day, showing a delayed outgrowth of TC-1-shPD-L1 tumors (Figure 16A). Since TC-1-shPD-L1 tumors remained small and in some mice even regressed, we used day 15 tumors to evaluate expression of PD-L1 on immune cells versus tumor cells, and to subsequently evaluate whether Nb C3 can accumulate in PD-L1 expressing tumors. Moreover, infiltration of CD8⁺ T-cells in these tumors and their expression of PD-1 was evaluated. Flow cytometry showed that all tumors were infiltrated with a comparable percentage of CD8⁺ T-cells and that these expressed similar high levels of PD-1 (data not shown). We further observed high expression of PD-L1 on TC-1-shPD-L1 tumor cells and on the immune cells that infiltrated these tumors, while the expression of PD-L1 was lower and comparable in TC-1 and TC-1-mPD-L1 tumors (Figure 16B). The high level of PD-L1 in mice transplanted with TC-1-shPD-L1 was confirmed in the SPECT/CT images and subsequent gamma counting of isolated tumors of mice injected with ^{99m}Tc-Nb C3 (Figure 16C-D).

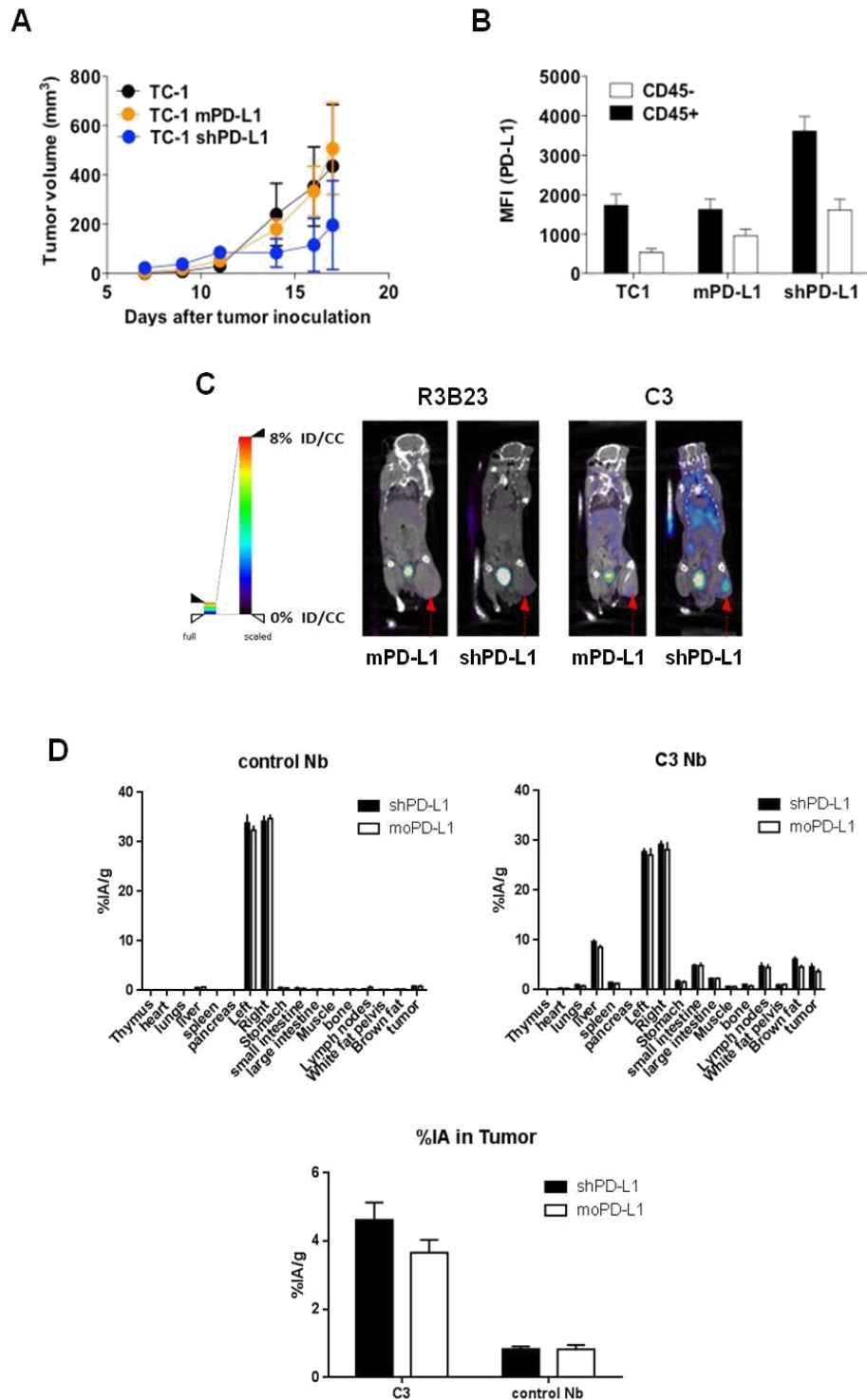


Figure 16: TC-1, TC-1-mPD-L1 or TC-1-shPD-L1 cells were injected on the back at the tail base of C57BL/6 mice. (A) Tumor growth was evaluated every other day. The evolution of the tumor size is shown as mean \pm SEM ($n = 1$, number of mice per condition = 5). (B) Mice were killed on day 12 and tumors were isolated, after which expression of PD-L1 on tumor cells (CD45⁻) and tumor-infiltrating immune cells (CD45⁺) was evaluated in flow cytometry ($n = 1$, number of mice per condition = 5). (C) Result of a representative SPECT/CT scan to determine biodistribution of ^{99m}Tc-Nb C3 injected in C57BL/6 mice bearing TC-1-mPD-L1 (left) or TC-1-shPD-L1 (right) tumors ($n = 1$, number of mice per condition = 6), (D) Results of the gamma counting of isolated organs from C57BL/6 mice bearing TC-1-mPD-L1 (white bar) or TC-1-shPD-L1 (black bar) tumors and injected with ^{99m}Tc-Nb C3 ($n = 1$, number of mice per condition = 6).

To avoid expression of PD-L1 on TC-1 tumor cells *in vivo*, we decided to take an alternative approach. TC-1 cells were transduced with lentiviral vectors that harbor CRISPR/Cas9, targeting DNA encoding mouse PD-L1. Down-regulation of PD-L1 on these TC-1 cells, referred to as TC-1-PD-L1^{-/-}, was demonstrated *in vitro* by flow cytometry. Moreover, TC-1-PD-L1^{-/-} cells were treated with IFN- γ to evaluate whether the expression of PD-L1 was abrogated even in the presence of a strong trigger (Figure 17).

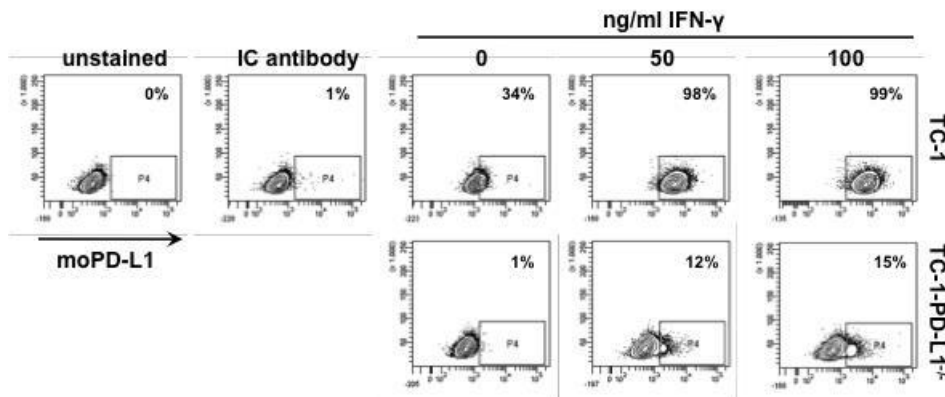


Figure 17: Expression of PD-L1 on TC-1 and TC-1-PD-L1^{-/-} treated or not with IFN- γ was evaluated in flow cytometry. The flow cytometry graphs are representative for one independent experiment (n = 1). The upper panel shows TC-1 cells, while the lower panel shows TC-1-PD-L1^{-/-} cells.

Subsequently, the TC-1 and TC-1-PD-L1^{-/-} cells were transplanted subcutaneously in C57BL/6 wild type or PD-L1^{-/-} mice. Tumor growth was followed up every other day, showing palpable tumors in all conditions on day 7. We observed that TC-1-PD-L1^{-/-} tumors rapidly regressed after day 7 irrespective of their growth in C57BL/6 wild type or PD-L1^{-/-} mice (Figure 18A). To evaluate whether this could be due to an adaptive immune response, we challenged these mice with TC-1 cells, showing lack of tumor growth, while inoculation of TC-1 cells in naïve mice resulted in tumor growth (data not shown). We also observed that growth of PD-L1 expressing TC-1 tumors was significantly delayed in C57BL/6 PD-L1^{-/-} mice when compared to their growth in wild type mice (Figure 18A). To evaluate whether the differences in growth can be correlated to differences in the tumor environment, we isolated TC-1 tumors from C57BL/6 wild type and PD-L1^{-/-} mice on day 22, and evaluated the expression of PD-L1 on the tumor cells and tumor-infiltrating immune cells in flow cytometry. In the C57BL/6 wild type mice, we observed that PD-L1 expression was high on tumor-infiltrating immune cells and low on tumor cells, while in the PD-L1^{-/-} mice an opposite pattern was observed (Figure 18B).

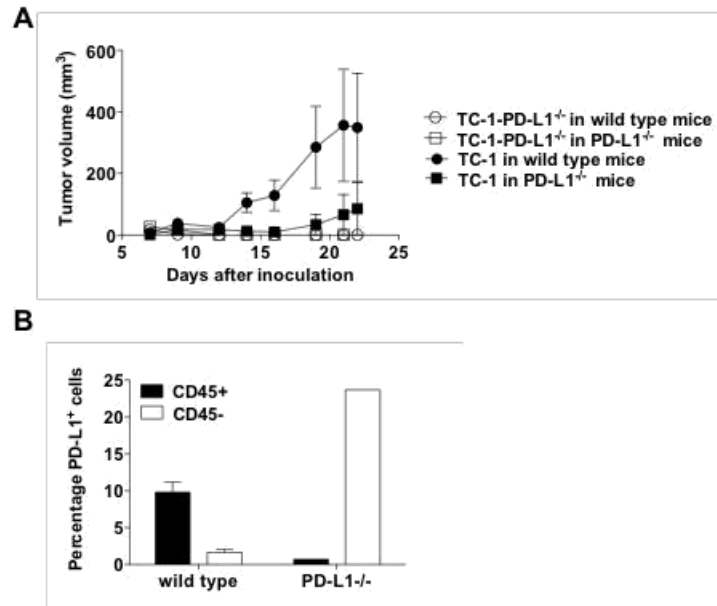


Figure 18: TC-1 and TC-1-PD-L1^{-/-} cells were injected on the back at the tail base of C57BL/6 wild type or PD-L1^{-/-} mice. (A) Tumor growth was evaluated every other day. The evolution of the tumor size is shown as mean \pm SEM (n = 1, number of mice per condition = 3). (B) Mice bearing TC-1 tumors were killed on day 22 and tumors were isolated, after which expression of PD-L1 on tumor cells (CD45⁻) and tumor-infiltrating immune cells (CD45⁺) was evaluated in flow cytometry (n = 1, number of mice per condition = 2).

These data suggest that absence of PD-L1 on tumor cells allows the immune system to counter tumor growth (Figure 18A). Moreover, tumor cells up-regulate PD-L1 to compensate for the absence of PD-L1 on immune cells (= adaptive resistance) (Figure 18B). Consequently, we did not obtain the conditions desired for imaging, i.e. a condition in which (i) we do not observe PD-L1 expression, (ii) only immune cells express PD-L1, (iii) only tumor cells express PD-L1 or (iv) both immune cells and tumor cells express PD-L1. To obtain such conditions, we will next evaluate tumor growth in immunodeficient mice and mice depleted of CD8⁺ T-cells.

Provided that tumors grow, we will allow restoration of the CD8⁺ T-cell population after which we will characterize expression of PD-L1 on tumor cells versus immune cells. In the assumption that we obtain the required conditions, we will subsequently grow tumors in CD8⁺ T-cell depleted mice and use these for imaging.

3. *In vitro* functional assays suggest that Nbs C3, C7 and E4, which specifically bind mouse PD-L1 are antagonists

3.1. Competition studies using the Biacore instruments show that Nbs C3, C7 and E4 can interrupt the PD-1/PD-L1 interaction, therefore can be considered blocking Nbs

To address whether the purified Nbs are able to block the natural binding between PD-L1 and its receptor PD-1, and as such could have therapeutic potential, competition studies were performed on the Biacore instruments by Nick Devoogdt. In this assay mPD-1Fc was immobilized, after which binding of mPD-L1Fc (at 25 nM concentration, which is the measured K_d value of the mPD-1Fc/mPD-L1Fc-interaction) mixed with variable concentrations of Nbs (C3, C7 and E4) was monitored. As the Nb concentration increases (0 to 400 nM), the RU representing binding between PD-1 and PD-L1 decreases, signifying inhibition of the PD-1/PD-L1 interaction. This inhibition was quantified by calculating the inhibitory concentration 50% (IC₅₀), in other words the Nb concentration at which PD-1/PD-L1 interaction is inhibited by a half. The lower IC₅₀ means the better inhibitor. All tested Nbs inhibited PD-1/PD-L1 interactions in this assay, albeit with different efficiencies (Table 5).

	C3	C7	E4
IC ₅₀	14.4	10.9	11.4
R-square	0.998	0.989	0.996

Table 5: The IC₅₀ and R-square were calculated based on the sensograms.

3.2. The presence of the blocking anti-PD-L1 mAb or the blocking anti-PD-L1 Nb C7 during antigen-presentation significantly enhances the stimulation of CD8⁺ T-cells

In order to analyze the effect of PD-L1/PD-1 interaction on the activation of T-cells during antigen presentation, we optimized a functional assay during which we co-cultured SIINFEKL pulsed mouse DCs, generated from bone marrow, with transgenic OT-I CD8⁺ T-cells which carry a TCR that recognizes the SIINFEKL peptide in the context of H2-K^b. Moreover, to evaluate if blockade of the PD-1/PD-L1 pathway could counteract its effect on T-cell activation we cultured the cells in the presence of blocking Nbs or mAbs specifically recognizing PD-L1. Flow cytometry was used to evaluate the expression of PD-L1 and CD80 on DCs and to evaluate the expression of PD-1, PD-L1 and CD80 on CD8⁺ T-cells prior and after the co-culture as well as on CD8⁺ T-cells that were stimulated with anti-CD3/anti-CD28 Ab coated beads. The DCs expressed both CD80 and PD-L1 (Figure 19A). Only a small percentage of the CD8⁺ T-cells before (Figure 19B) and after co-culture (data not shown) with DCs expressed CD80, PD-L1 and PD-1, while these markers were up-regulated upon stimulation with the anti-CD3/anti-CD28 Ab coated beads (Figure 19B). After 48 hours of co-culture, we evaluated the production of TNF-α and IFN-γ by the CD8⁺ T-cells in flow cytometry. Despite the low expression of CD80, PD-L1 and PD-1 on the CD8⁺ T-cells,

we observed that the presence of blocking anti-PD-L1 mAbs or the anti-PD-L1 Nb C7 during antigen presentation significantly enhances the cytokine production by CD8⁺ T-cells compared to their controls, thus improving their functionality.

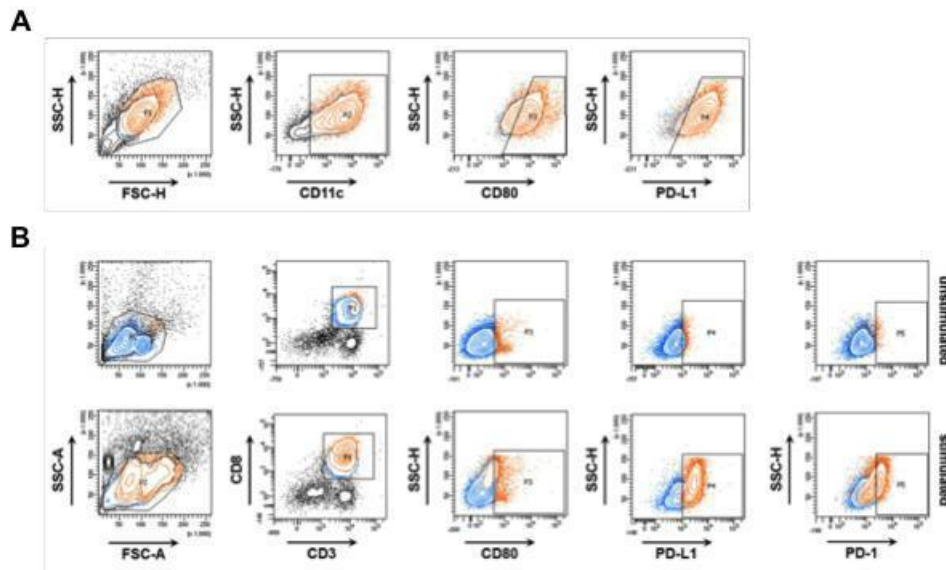


Figure 19: Phenotype of the DCs and CD8⁺ OT-I cells used in the functional assay. Flow cytometry was performed to evaluate the phenotype of DCs and CD8⁺ OT-I cells before the start of the co-culture. DCs were stained with Abs specific for CD11c, CD80 and PD-L1, while T-cells were stained with Abs specific for CD3, CD8, CD80, PD-L1 and PD-1. The graphs in A represent the gating strategy used to evaluate the expression of CD80 and PD-L1 on CD11c⁺ cells. The graphs in B represent the gating strategy used to evaluate the expression of CD80, PD-L1 and PD-1 on CD3⁺ and CD8⁺ T-cells. The upper panel shows the phenotype of unstimulated cells, while the lower panel shows the phenotype of T-cells stimulated with anti-CD3/anti-CD28 Ab coated beads (n = 4).

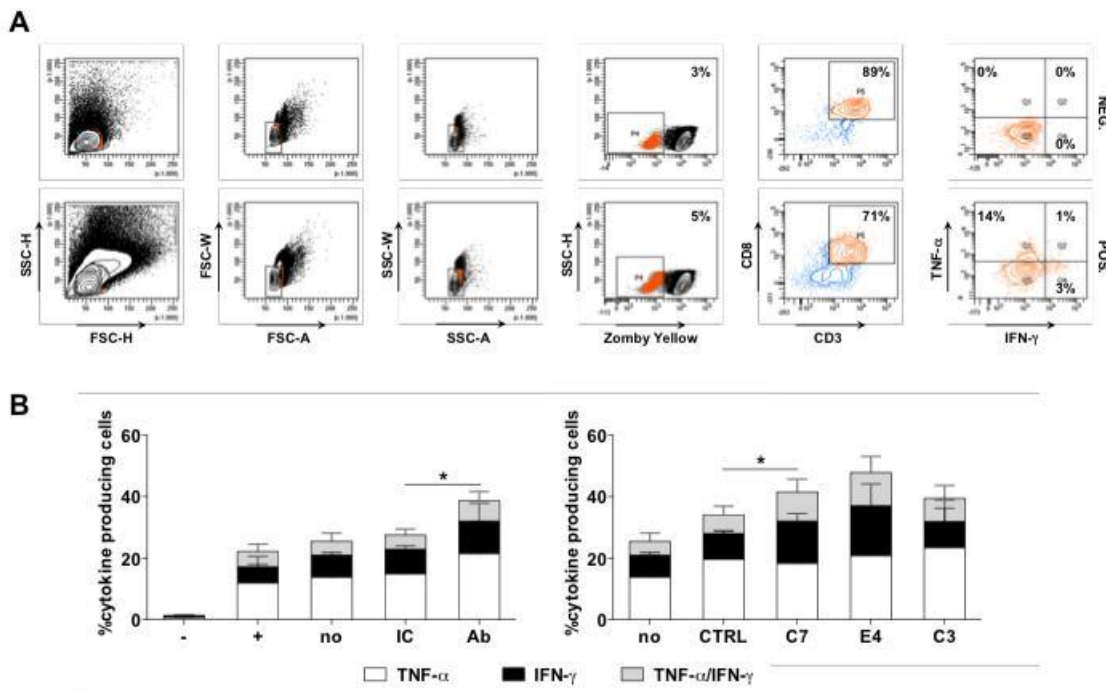


Figure 20: The production of cytokines by CD8⁺ OT-I cells is significantly enhanced in the presence of mAb or Nb C7. (A) Flow cytometry was performed to evaluate the production of TNF- α and IFN- γ . Representative FACS plots showing the gating strategy are depicted (n = 3). (B) The graphs summarize the results of 3 independent experiments (n = 3).

3.3. The presence of the blocking mAbs or blocking Nbs during tumor cell-CD8⁺ T-cell interactions does not significantly affect the viability of tumor cells or CD8⁺ T-cells

In order to evaluate the influence of PD-1/PD-L1 interaction on the viability of tumor cells and tumor specific T-cells, we co-cultured CD8⁺ OT-I cells, which were either stimulated or not with anti-CD3/anti-CD28 Ab coated beads with TC-1-mPD-L1 or TC-1-PD-L1^{-/-} cells, which were either pulsed or not with SIINFEKL. Additionally, we also evaluated if the effect of PD-1/PD-L1 interaction on the viability of cells could be counteracted using anti-PD-L1 Nbs C3, C7 and E4 or anti-PD-L1 mAbs. Prior to the co-culture, flow cytometry was performed to analyze the expression of CD80 and PD-L1 on the TC-1 cells, showing absence of PD-L1 on TC-1-PD-L1^{-/-} but not on TC-1-mPD-L1 cells, while both cell types expressed high levels of CD80 (Figure 21). The phenotype of the CD8⁺ T-cells is shown in Figure 19B.

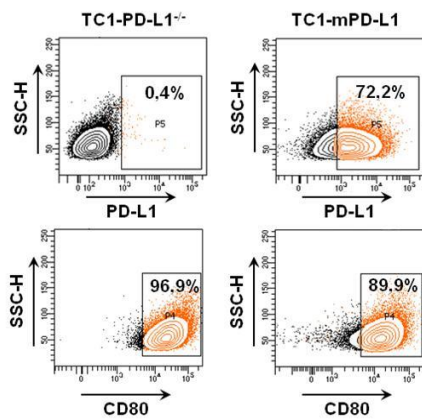


Figure 21: PD-L1 and CD80 expression on TC-1-PD-L1^{-/-} and TC-1-mPD-L1 cells. The upper panel shows the cells stained with anti-PD-L1 Abs, while the lower panel shows the cells stained with anti-CD80 Abs.

After 18 hours of co-culture, we stained the cells with an anti-CD45 Ab to discriminate immune cells (CD45⁺) from tumor cells (CD45⁻), after which we performed an Annexin-V and 7-AAD staining to evaluate the percentage of dead cells in these cell populations (Figure 22A). For the analysis, the percentage of dead cells was normalized to the percentage of cell death observed when T-cells or tumor cells were cultured separately. Furthermore, the effect of TCR triggering was taken into account in the analysis by comparing the percentage of cell death in cultures with SIINFEKL pulsed versus unpulsed cells. We observed that the viability of unstimulated T-cells (low expression of CD80, PD-L1 and PD-1) or stimulated T-cells (high expression of CD80, PD-L1 and PD-1) was not affected by the presence of PD-L1 on the TC-1 cells (Figure 22B). We did observe that the viability of activated T-cells in the co-cultures was significantly lower than the viability of unstimulated cells irrespective of the presence or absence of PD-L1 on the TC-1 cells (Figure 22B). We further observed that the tumor cell viability was lower in the co-cultures with activated T-cells than in cultures with unstimulated T-cells both for the TC-1-mPD-L1 as the TC-1-PD-L1^{-/-} cells (Figure 22B). The inclusion of anti-PD-L1 blocking mAbs or Nbs did not significantly affect the viability of the T-cells or tumor cells (Figure 22B).

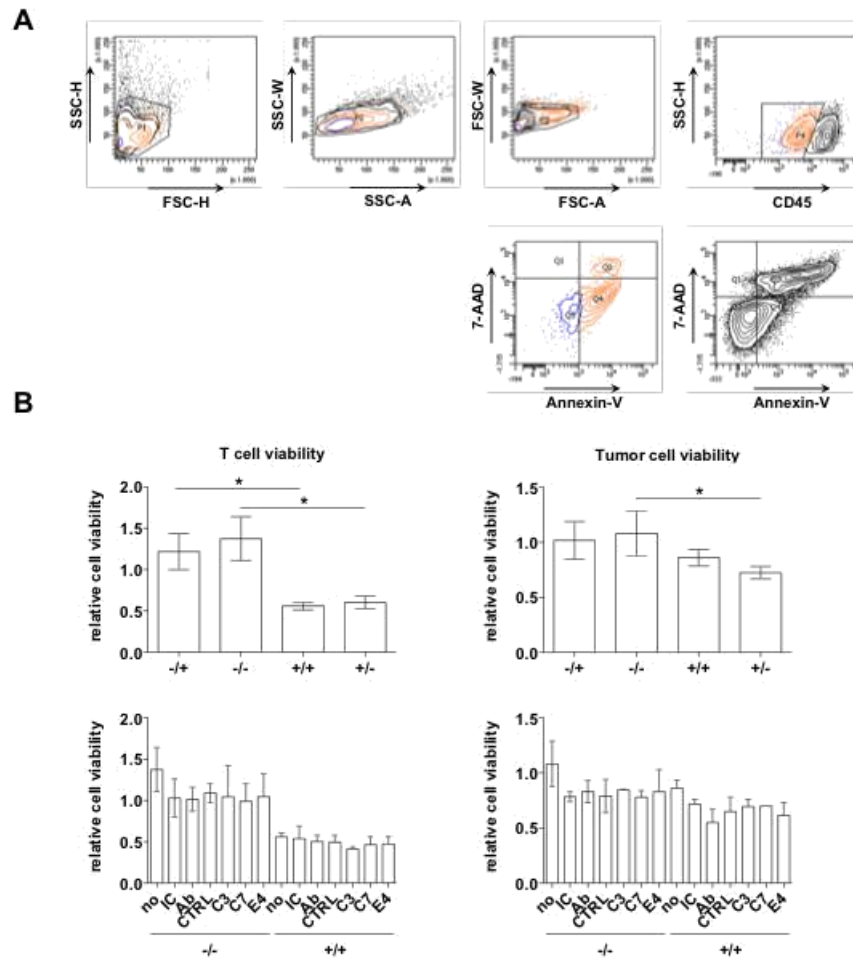


Figure 22: Viability of the tumor cells and CD8⁺ T-cells. Flow cytometry was performed to evaluate the viability of T-cells and TC-1 cells, when co-cultured for 24 hours in the presence or not of anti-PD-L1 Nbs or mAbs. (A) Gating strategy of the flow cytometry analysis. (B) Graphs summarizing the results of 5 (upper panel) and 2 (lower panel) independent experiments. Herein -/-, -/+, +/- and +/+ signify the results of co-cultures between unstimulated T-cells and TC-1-PD-L1^{-/-} cells, unstimulated T-cells and TC-1-mPD-L1 cells, stimulated T-cells and TC-1-PD-L1^{-/-} cells and stimulated T-cells and TC-1-mPD-L1 cells.

3.4. The presence of the blocking anti-PD-L1 mAbs during tumor cell-CD8⁺ T-cell interactions significantly enhances the functionality of the CD8⁺ T-cells

Using the same cells from the functional assay described above, we evaluated if PD-1/PD-L1 interaction could affect the functionality of stimulated or unstimulated CD8⁺ OT-I cells when cultured for 48 hours with PD-L1⁻ or PD-L1⁺ TC-1 cells. Flow cytometry was used to measure the production of TNF- α and IFN- γ by the T-cells. To our surprise we observed that the presence of mAbs in the co-culture of unstimulated T-cells (low expression of CD80, PD-L1 and PD-1) with TC-1-PD-L1^{-/-} convincingly enhanced the production of cytokines by these T-cells (Figure 23A), while the presence of mAbs only marginally affected the cytokine production in the co-culture of stimulated T-cells (high expression of CD80, PD-L1 and PD-1) with TC-1 cells (PD-L1⁺) (Figure 23B). Moreover, addition of blocking Nbs C3, C7 or E4 had no impact on cytokine production (Figure 23A and B).

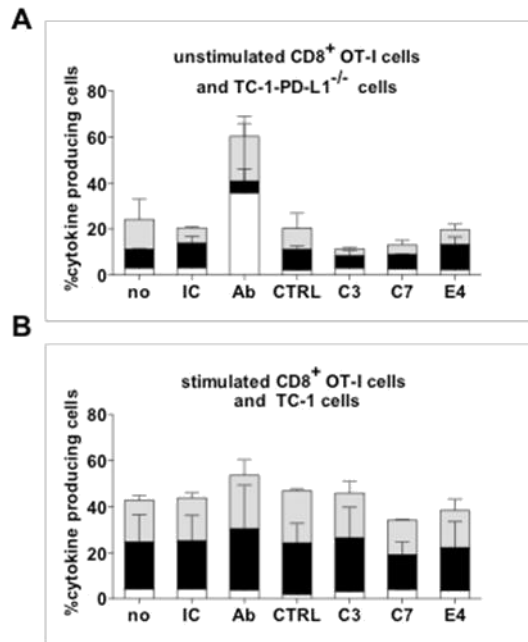


Figure 23: The functionality of unstimulated CD8⁺ T-cells is enhanced in the presence of blocking anti-PD-L1 mAbs. CD8⁺ OT-I cells, which were either stimulated or not with anti-CD3/anti-CD28 Ab coated beads were co-cultured with antigen-presenting TC-1-mPD-L1 or TC-1-PD-L1^{-/-} respectively. Two days after the start of the co-culture, we evaluated the production of TNF- α and IFN- γ by the T-cells in flow cytometry. The same gating strategy as shown in figure 20A was used. The graphs in (A) and (B) summarize the results of the co-cultures between (A) unstimulated CD8⁺ OT-I cells and TC-1-PD-L1^{-/-} cells and (B) stimulated CD8⁺ OT-I cells and TC-1 (PD-L1⁺) cells (n = 2).

DISCUSSION

Immune checkpoint blockade using mAbs has been recently accepted as a successful strategy in cancer immunotherapy. The most broadly studied immune checkpoint pathways are the CTLA-4/B7 and PD-1/PD-L1 pathways, which are proven to play a role in dampening antitumor T-cell activity in cancer patients. Importantly, blockade of inhibitory signals provided by the PD-1/PD-L1 pathway has shown to enhance T-cell activity accompanied with significantly less toxicity and adverse events compared to blockade of the CTLA-4/B7 pathway. Additionally, compared to many other treatments, the blockade of PD-1/PD-L1 signaling has shown to induce prolonged off-treatment therapeutic responses. Immune checkpoint blockade has thus been considered by many to be a disruptive innovation, meaning that this modern therapy will eventually predominate the existing market and value network. However, this is not a strict definition because, in truth, immune checkpoint blockade is far from taking over the entire „market“ of patients with cancer. This can be explained by the fact that currently only a subset of patients shows beneficial responses during clinical trials, usually around 30%. Moreover, in more than half of the patients, treatment is associated with toxic adverse events without any benefits. Similarly, other immunotherapies, like adoptive T-cell transfer and DC vaccination, show promising results in only a subset of cancer patients^{93,94}. Therefore, combining different cancer immunotherapies may increase their individual benefit. Consequently, there is a strong need to further invest in research to ensure a better overall outcome.

During this thesis, we aimed to improve current immune checkpoint blockade therapy by using Nbs, specific for the inhibitory ligand PD-L1. We evaluated the theranostic value of the Nbs by screening them for both tumor stratification and therapy. We believe that it is of utmost importance to identify patients that are eligible for treatment with PD-1/PD-L1 targeting drugs. Moreover, we believe that mAbs, which are currently evaluated to image PD-1 or PD-L1 expression might not be the best tool for these purposes, as they can be immunogenic and show sub-optimal targeting and pharmacokinetic properties⁸². In contrast, Nbs are non-immunogenic, show good targeting and pharmacokinetic traits and are relatively easy to radiolabel, which make them an attractive candidate for imaging of immune checkpoints in the tumor environment⁹⁵. Moreover, Nbs might be a better candidate for therapy purposes as well, since they can more easily penetrate tumor tissue when compared to mAbs, and if desired we can enhance the Nbs avidity for its target by linking two identical

Nbs into an „antibody-like“ bivalent format⁹⁶.

In this study, we focused on Nbs specific for PD-L1. Even though mAbs against PD-1 are at the centre of attention in the clinic, we decided to work with the ligand PD-L1 because of its critical role in tumor progression. Overexpression of PD-L1 is a potent facilitator for tumor growth and metastasis⁹⁷. Our observations indeed showed that expression of PD-L1 on tumor cells and/or immune cells is a critical factor that determines tumor progression, since TC-1-PD-L1^{-/-} cells did not grow in wild type or PD-L1^{-/-} mice and as TC-1 cells showed a reduced growth in PD-L1^{-/-} mice (Figure 18A). Not surprisingly, PD-L1 has shown promise as a biomarker, predictive for the therapy response to anti-PD-1 and anti-PD-L1 therapy⁹⁸.

Another reason why we preferred to target PD-L1 is because it provides negative signals to among others effector T cells by interacting with PD-1 as well as CD80. Antagonistic agents

targeted to PD-L1 could prevent both of these interactions and as such tackle two inhibitory signaling pathways. Our experiments indeed suggest that blocking of CD80-mediated negative signaling is relevant, since we observed that mAbs targeting PD-L1 enhanced the activity of T cells both in the DC-T cell (Figure 20B) as tumor cell-T cell co-cultures (Figure 23), even if the T cells are negative for PD-1. Interestingly, we observed that these T cells do express low levels of CD80 and PD-L1. These data suggest that PD-L1 in these assays triggers negative signaling via a PD-1 independent, most likely CD80 pathway. These observations indicate that targeting PD-L1 instead of PD-1 might be a more promising strategy for future cancer immunotherapies.

We evaluated 42 Nbs, directed against the inhibitory receptor ligand PD-L1, that were available at the CMIM lab. We selected and characterized 3 different Nbs (C3, C7 and E4) that show high specificity and affinity for the mouse PD-L1 protein, and moreover bind to human PD-L1, albeit with a lower affinity. In order to analyze the applicability of Nbs C3, C7 and E4 for imaging, we started with evaluating the biodistribution of these purified Nbs that were radiolabeled and systemically injected in either wild type or PD-L1^{-/-} C57BL/6 mice. For all Nbs there is typically a high uptake in kidneys and bladder because of their renal elimination. Moreover, we observed that Nb E4 and C3, showed the expected biodistribution. However, there is a prominent presence of background signal in the liver in PD-L1^{-/-} mice for all 3 Nbs, which at this point cannot be explained (Figure 11-14). As the PD-L1^{-/-} mice were genotyped before their use, we can conclude that the signal observed in PD-L1^{-/-} mice is not PD-L1 specific.

In order to evaluate the accumulation of the selected Nbs in the tumor environment, we inoculated wild type mice with TC-1 tumor cells that were lentivirally modified to either up- or down-regulate expression of PD-L1. Down-regulation of PD-L1 was accomplished at least *in vitro* using RNA interference (Figure 15). Surprisingly, after imaging of these mice using the radiolabeled Nb C3, we observed a higher uptake of the Nb at tumor site in mice inoculated with TC-1-shPD-L1 cells compared to mice inoculated with TC-1-mPD-L1 cells (Figure 15C-D). These results were confirmed after analyzing the expression of PD-L1 on isolated tumor cells and tumor-infiltrating immune cells using flow cytometry (Figure 15B). This observation can be explained by the fact that infiltration of the TC-1-shPD-L1 tumors with T cells can induce the production of PD-L1-inducing cytokines like for example IFN- γ . This might have triggered continuous and high transcription of the PD-L1 gene, resulting in an “overload” of PD-L1 mRNA. It is plausible that the expression of shRNA to target these transcripts to the RISC complex for degradation was insufficient to eliminate all PD-L1 mRNA molecules, hence resulting in expression of PD-L1. Initial infiltration of TC-1-shPD-L1 tumors with IFN- γ producing T cells would moreover explain the slower growth of these tumors *in vivo* when compared to TC-1 tumors (Figure 15A). Additionally, an equilibrium phase could be reached later on as a consequence of what may be considered as adaptive immune resistance. Previous studies already suggested that infiltrating immune cells indeed have the capacity to produce factors driving the expression of PD-L1 as a negative feedback mechanism⁵². Interestingly, we observed that PD-L1 expression was also higher on immune cells residing in TC-1-shPD-L1 isolated tumors compared to TC-1-mPD-L1 tumors, suggesting that

immune cells could compensate for the initial lack of PD-L1 on tumor cells. The PD-L1 expression observed on both tumor and tumor residing immune cells can improve their immune suppressive activity and capacity to evade eradication by an anticancer immune response. This brings forth the importance of immunomodulatory molecules expressed by cells in the tumor microenvironment. Taken together, these findings help to explain why the inoculated TC-1-shPD-L1 tumor cells were able to express high levels of PD-L1, whereas prior to inoculation the expression of PD-L1 could be efficiently blocked by RNA interference. Importantly, from these experiments we can conclude that Nb C3 specifically accumulates in sites with PD-L1 expression, and that the signals obtained seem to reveal the level of PD-L1 expression.

Because of the inadequate capacity of shRNA to block PD-L1 expression on TC-1 cells *in vivo*, we decided to use the CRSIPR/Cas9 gene editing technology. The delivery of Cas9 protein and appropriate guide RNA (targeting PD-L1) will lead to the excision of PD-L1 in the cell's genome, making it impossible for the cell to express PD-L1. The many advantages linked to the use of this tool has led to the AAAS's award for scientific breakthrough in 2015⁹⁹. We first analyzed the efficiency of 3 different guide RNA molecules to knock out the expression of PD-L1 in TC-1 cells. Only one guide RNA was able to reduce the expression of PD-L1 below the detection limit. The resulting cells are further referred to as TC-1-PD-L1^{-/-} (Figure 17). Next, we inoculated the TC-1-PD-L1^{-/-} cells, and TC-1 cells in wild type or PD-L1^{-/-} C57BL/6 mice to follow up tumor growth over time. Surprisingly, after the observation of a palpable tumor at day 7, all mice inoculated with TC-1-PD-L1^{-/-} cells showed tumor regression (Figure 18A). These observations suggest that the complete absence of PD-L1 on tumor cells, even after the exposure to PD-L1 inducing cytokines, had a tremendous effect on the growth of these cells compared to the growth of PD-L1 positive tumor cells. Moreover, we re-inoculated TC-1 cells into these tumor-free mice and couldn't observe tumor growth, suggesting that a tumor specific adaptive immune response was generated upon inoculation of TC-1-PD-L1^{-/-} tumor cells, which was able to protect the mice against a re-challenge with TC-1 cells. Although these findings are interesting from an immunological point of view, it poses a hurdle for our imaging purposes. In future, we will grow TC-1 and TC-1-PD-L1^{-/-} tumors in immunodeficient mice, evaluating their growth in the absence of immune cells. Provided that tumors grow, we will use this system for imaging. Moreover, to obtain the conditions desired for imaging, i.e. a condition in which (i) we do not observe PD-L1 expression, (ii) only immune cells express PD-L1, (iii) only tumor cells express PD-L1 or (iv) both immune cells and tumor cells express PD-L1, we will also evaluate tumor growth in mice depleted of CD8⁺ T cells (using mAbs). If TC-1-PD-L1^{-/-} tumors grow after depletion of CD8⁺ T cells, we have a proof that CD8⁺ T cells hamper the growth of these tumors. Moreover, when tumors have a reasonable size for imaging, we can allow restoration of the CD8⁺ T cell population by no longer using depleting mAbs, after which we can evaluate the expression of PD-L1 on tumor cells versus immune cells. In the assumption that we obtain the required conditions, we can proceed with our imaging studies.

Next to the imaging studies, we evaluated whether the purified Nbs are able to block the natural binding of PD-L1 to its receptor PD-1, and as such address the therapeutic potential.

Competition studies on the Biacore instruments were previously performed and suggested a good blocking capacity of Nb C3, C7 and E4. Therefore, we set up different functional assays for the evaluation of these Nbs. As PD-L1 on tumor cells is described to protect them from T-cell mediated killing, and as PD-1 on T cells has been linked to their removal by cell death induction²⁹, we evaluated the viability of tumor cells and T cells co-cultured under various conditions (Figure 22B). We observed that the viability of TC-1 tumor cells was lower in co-cultures with CD8⁺ T cells, activated with anti-CD3/anti-CD28 Ab coated beads resulting in the up-regulation of PD-1, albeit irrespective of PD-L1 expression. However, this also resulted in a lower viability of the T cells themselves. The viability of tumor cells in co-cultures with unstimulated, therefore PD-1⁻ T cells, was significantly higher. Again the expression of PD-L1 on tumor cells did not affect the cell viability of tumor cells or T cells. This observation suggests that when T cells are not properly stimulated, they are unable to efficiently eradicate tumor cells. Moreover, in this assay there is no evidence for a protection of tumor cells or reduction of T-cell viability upon PD-1/PD-L1 interaction. Not surprisingly, PD-L1 blockade did not influence the viability of CD8⁺ T cells nor TC-1 tumor cells. However, during the functional assays we did observe that PD-L1 blockade mediated by a mAb could enhance the stimulation of CD8⁺ T cells during antigen presentation by both DCs (Figure 20) and tumor cells (Figure 23). Conversely, in the DC-T cell co-culture, the CD8⁺ T cells did not express PD-1, which puts us in doubt whether the PD-1/PD-L1 pathway is truly the one we were targeting here. A second binding partner of PD-L1 is CD80 and its interaction has previously been shown to have a functional significance³⁸. Signals through PD-L1 and CD80 are inhibitory, decrease T-cell proliferation and block cytokine production. This compels a revised view of the interaction between molecules within the B7/CD28 family in the regulation of T-cell activity. Interestingly, during co-culture assays using tumor cells, we observed a convincingly enhanced functionality of unstimulated, therefore PD-1⁻ T cells in co-culture with TC1-PDL1^{-/-} tumor cells when using a mAb against PD-L1. Surprisingly, we observed high expression levels of CD80 on tumor cells and a certain level of PD-L1 on T cells. It is likely that these proteins could have interacted during the co-culture and downstream influenced the functionality of the CD8⁺ T cells in accordance with the literature described above. Little is known about the capacity of the anti-PD-L1 mAb to block binding of PD-L1 to CD80. This is surely interesting to investigate in the future. Moreover, it would be worthwhile to use the functional assays described in this thesis to evaluate the effect of anti-CD80 and anti-PD-1 mAbs, as this will shed light on potential mechanisms of negative signaling. Finally, when stimulated PD-1⁺ T cells were co-cultured with TC-1-mPD-L1 (PD-L1⁺) cells we only observed a small increase in their functionality, suggesting that the mAbs used in this study are not potent enough to block the negative signals provided by interaction between PD-1 and PD-L1.

The blockade of PD-L1 using Nbs was shown to enhance the functionality of T cells when in co-culture with DCs but not with TC-1 tumor cells (Figure 20B). This might be explained by the fact that DCs are professional antigen-presenting cells that can provide a number of co-stimulatory signals (e.g. CD86, OX40L, 4-1BBL, etc) and stimulatory cytokines (e.g. IL-12), next to the negative signals triggered by PD-L1, while tumor cells are less likely to express

the co-stimulatory molecules. Moreover, it might be that the monovalent format of the Nbs is not optimal to block the PD-L1/PD-1 pathway efficiently. Therefore, we suggest in future evaluating the use of multivalent Nbs, which consists of two or more Nbs linked to each other. As a consequence of multiple antigen-binding units, we can expect that multivalent Nbs will have a higher avidity to PD-L1. As such we can potentially increase their therapeutic window.

In conclusion, our current findings suggest that Nbs, which specifically bind PD-L1 can be used for imaging purposes. Additionally, Nb-mediated blockade of the inhibitory receptor ligand PD-L1 resulted in enhanced functionality of T cells co-cultured with DCs. These preliminary findings warrant further research into the use of Nbs as theranostics.

ACKNOWLEDGEMENTS

From the moment I knew that I would do my internship at LMCT, it was clear to me it would be very important to try my very best. Because of the stimulating atmosphere and motivated researchers surrounding me, it was not surprising I was able to do so.

First, I want to thank Katrijn Broos for supervising me during the past 9 months. She taught me many different techniques that I will hopefully use during the rest of my career. Starting with the generation of lentiviral vectors, flow cytometry and linked herewith its analysis to the production of Nbs, all the different *in vitro* assays and the exciting *in vivo* studies. I hope that at some point in the future I will possess as many skills and knowledge as she does.

My special thanks go out to professor Karine Breckpot for granting me the possibility of doing my thesis under her supervision. During this internship, my love for research has grown tremendously as has my respect for her.

Next, I want to thank professor Nick Devoogdt and Marleen Keyaarts for being co-promotors during my project.

My interest for immunology initially started during the lessons of professor Kris Thielemans, to whom I owe a lot of respect.

Additionally, this year would not have been the same without the interesting conversations and enjoyable times with colleagues from the lab during and after work.

It was a pleasure and inspiration working with you all!

I want to thank my parents and siblings for giving me all the support and positive stimuli throughout this busy year.

I am also grateful to my girlfriend, Annika, for being the best support during my education and this final thesis year. Thank you for always believing in me.

At last I want to thank all my friends from the VUB, all the great people I met last year during my internship in Sheffield and the two other members from "The 3 Jackies" for making me the person who I've become.

REFERENCES

1. Coulie, P. G.; Van den Eynde, B. J.; van der Bruggen, P.; Boon, T., Tumour antigens recognized by T lymphocytes: at the core of cancer immunotherapy. *Nat Rev Cancer* **2014**, *14* (2), 135-46.
2. Smyth, M. J.; Dunn, G. P.; Schreiber, R. D., Cancer immunosurveillance and immunoediting: the roles of immunity in suppressing tumor development and shaping tumor immunogenicity. *Adv Immunol* **2006**, *90*, 1-50.
3. Motz, G. T.; Coukos, G., Deciphering and reversing tumor immune suppression. *Immunity* **2013**, *39* (1), 61-73.
4. Mauge, L.; Terme, M.; Tartour, E.; Helley, D., Control of the adaptive immune response by tumor vasculature. *Front Oncol* **2014**, *4*, 61.
5. Gobert, M.; Treilleux, I.; Bendriss-Vermare, N.; Bachelot, T.; Goddard-Leon, S.; Arfi, V.; Biota, C.; Doffin, A. C.; Durand, I.; Olive, D.; Perez, S.; Pasqual, N.; Faure, C.; Ray-Coquard, I.; Puisieux, A.; Caux, C.; Blay, J. Y.; Menetrier-Caux, C., Regulatory T cells recruited through CCL22/CCR4 are selectively activated in lymphoid infiltrates surrounding primary breast tumors and lead to an adverse clinical outcome. *Cancer Res* **2009**, *69* (5), 2000-9.
6. De Vlaeminck, Y.; González-Rascón, A.; Goyvaerts, C.; Breckpot, K., Cancer-associated myeloid regulatory cells. *Frontiers in Immunology* **2016**, *7*.
7. Van Overmeire, E.; Laoui, D.; Keirsse, J.; Van Ginderachter, J. A.; Sarukhan, A., Mechanisms driving macrophage diversity and specialization in distinct tumor microenvironments and parallelisms with other tissues. *Front Immunol* **2014**, *5*, 127.
8. Marvel, D.; Gabrilovich, D. I., Myeloid-derived suppressor cells in the tumor microenvironment: expect the unexpected. *J Clin Invest* **2015**, *125* (9), 3356-64.
9. Gajewski, T. F., Identifying and overcoming immune resistance mechanisms in the melanoma tumor microenvironment. *Clin Cancer Res* **2006**, *12* (7 Pt 2), 2326s-2330s.
10. Aarntzen, E. H.; Schreiber, G.; Bol, K.; Lesterhuis, W. J.; Croockewit, A. J.; de Wilt, J. H.; van Rossum, M. M.; Blokx, W. A.; Jacobs, J. F.; Duiveman-de Boer, T.; Schuurhuis, D. H.; Mus, R.; Thielemans, K.; de Vries, I. J.; Figdor, C. G.; Punt, C. J.; Adema, G. J., Vaccination with mRNA-electroporated dendritic cells induces robust tumor antigen-specific CD4+ and CD8+ T cells responses in stage III and IV melanoma patients. *Clin Cancer Res* **2012**, *18* (19), 5460-70.
11. Van der Jeught, K.; Bialkowski, L.; Daszkiewicz, L.; Broos, K.; Goyvaerts, C.; Renmans, D.; Van Lint, S.; Heirman, C.; Thielemans, K.; Breckpot, K., Targeting the tumor microenvironment to enhance antitumor immune responses. *Oncotarget* **2015**, *6* (3), 1359-81; Marabelle, A.; Kohrt, H.; Caux, C.; Levy, R., Intratumoral immunization: a new paradigm for cancer therapy. *Clin Cancer Res* **2014**, *20* (7), 1747-56.
12. Vasaturo, A.; Di Blasio, S.; Peeters, D. G.; de Koning, C. C.; de Vries, J. M.; Figdor, C. G.; Hato, S. V., Clinical Implications of Co-Inhibitory Molecule Expression in the Tumor Microenvironment for DC Vaccination: A Game of Stop and Go. *Front Immunol* **2013**, *4*, 417.
13. Corthay, A., A three-cell model for activation of naive T helper cells. *Scand J Immunol* **2006**, *64* (2), 93-6.
14. Pennock, N. D.; White, J. T.; Cross, E. W.; Cheney, E. E.; Tamburini, B. A.; Kedl, R. M., T cell responses: naive to memory and everything in between. *Adv Physiol Educ* **2013**, *37* (4), 273-83.
15. Wing, K.; Sakaguchi, S., Regulatory T cells exert checks and balances on self tolerance and autoimmunity. *Nat Immunol* **2010**, *11* (1), 7-13.
16. Marquez-Rodas, I.; Cerezuela, P.; Soria, A.; Berrocal, A.; Riso, A.; Gonzalez-Cao, M.; Martin-Algarra, S., Immune checkpoint inhibitors: therapeutic advances in melanoma. *Ann Transl Med* **2015**, *3* (18), 267.
17. Capece, D.; Verzella, D.; Fischietti, M.; Zazzeroni, F.; Alesse, E., Targeting costimulatory molecules to improve antitumor immunity. *J Biomed Biotechnol* **2012**, *2012*, 926321; Krummel, M. F.; Allison, J. P., CTLA-4 engagement inhibits IL-2 accumulation and cell cycle progression upon activation of resting T cells. *J Exp Med* **1996**, *183* (6), 2533-40; Walunas, T. L.; Bakker, C. Y.; Bluestone, J. A., CTLA-4 ligation blocks CD28-dependent T cell activation. *J Exp Med* **1996**, *183* (6), 2541-50.

REFERENCES

18. Quezada, S. A.; Peggs, K. S.; Curran, M. A.; Allison, J. P., CTLA4 blockade and GM-CSF combination immunotherapy alters the intratumor balance of effector and regulatory T cells. *J Clin Invest* **2006**, *116* (7), 1935-45.
19. Li, N.; Wang, Y.; Forbes, K.; Vignali, K. M.; Heale, B. S.; Saftig, P.; Hartmann, D.; Black, R. A.; Rossi, J. J.; Blobel, C. P.; Dempsey, P. J.; Workman, C. J.; Vignali, D. A., Metalloproteases regulate T-cell proliferation and effector function via LAG-3. *Embo j* **2007**, *26* (2), 494-504.
20. Huang, C. T.; Workman, C. J.; Flies, D.; Pan, X.; Marson, A. L.; Zhou, G.; Hipkiss, E. L.; Ravi, S.; Kowalski, J.; Levitsky, H. I.; Powell, J. D.; Pardoll, D. M.; Drake, C. G.; Vignali, D. A., Role of LAG-3 in regulatory T cells. *Immunity* **2004**, *21* (4), 503-13; Joosten, S. A.; van Meijgaarden, K. E.; Savage, N. D.; de Boer, T.; Triebel, F.; van der Wal, A.; de Heer, E.; Klein, M. R.; Geluk, A.; Ottenhoff, T. H., Identification of a human CD8+ regulatory T cell subset that mediates suppression through the chemokine CC chemokine ligand 4. *Proc Natl Acad Sci U S A* **2007**, *104* (19), 8029-34.
21. Liang, B.; Workman, C.; Lee, J.; Chew, C.; Dale, B. M.; Colonna, L.; Flores, M.; Li, N.; Schweighoffer, E.; Greenberg, S.; Tybulewicz, V.; Vignali, D.; Clynes, R., Regulatory T cells inhibit dendritic cells by lymphocyte activation gene-3 engagement of MHC class II. *J Immunol* **2008**, *180* (9), 5916-26.
22. Macon-Lemaitre, L.; Triebel, F., The negative regulatory function of the lymphocyte-activation gene-3 co-receptor (CD223) on human T cells. *Immunology* **2005**, *115* (2), 170-8; Sega, E. I.; Leveson-Gower, D. B.; Florek, M.; Schneidawind, D.; Luong, R. H.; Negrin, R. S., Role of lymphocyte activation gene-3 (Lag-3) in conventional and regulatory T cell function in allogeneic transplantation. *PLoS One* **2014**, *9* (1), e86551; Hemon, P.; Jean-Louis, F.; Ramgolam, K.; Brignone, C.; Viguier, M.; Bachelez, H.; Triebel, F.; Charron, D.; Aoudjit, F.; Al-Daccak, R.; Michel, L., MHC class II engagement by its ligand LAG-3 (CD223) contributes to melanoma resistance to apoptosis. *J Immunol* **2014**, *186* (9), 5173-83.
23. Anderson, A. C., Tim-3, a negative regulator of anti-tumor immunity. *Curr Opin Immunol* **2012**, *24* (2), 213-6.
24. Kleponis, J.; Skelton, R.; Zheng, L., Fueling the engine and releasing the break: combinational therapy of cancer vaccines and immune checkpoint inhibitors. *Cancer Biol Med* **2015**, *12* (3), 201-8; da Silva Correia, J.; McNeeley, P.; Do, M.; Altobelli, L.; Chhoa, M.; Tomlinson, G.; Sheffer, J.; Kehry, M.; Marino, M.; Laken, H.; King, D., Identification and Characterization of a Potent Anti-Human TIM-3 Antagonist. In *AACR, Orlando, 2014*; Blank, C. U., The perspective of immunotherapy: new molecules and new mechanisms of action in immune modulation. *Curr Opin Oncol* **2014**, *26* (2), 204-14; Couzin-Frankel, J., Breakthrough of the year 2013. Cancer immunotherapy. *Science* **2013**, *342* (6165), 1432-3.
25. Topalian, S. L.; Drake, C. G.; Pardoll, D. M., Immune checkpoint blockade: a common denominator approach to cancer therapy. *Cancer Cell* **2015**, *27* (4), 450-61.
26. Hodi, F. S.; O'Day, S. J.; McDermott, D. F.; Weber, R. W.; Sosman, J. A.; Haanen, J. B.; Gonzalez, R.; Robert, C.; Schadendorf, D.; Hassel, J. C.; Akerley, W.; van den Eertwegh, A. J.; Lutzky, J.; Lorigan, P.; Vaubel, J. M.; Linette, G. P.; Hogg, D.; Ottensmeier, C. H.; Lebbe, C.; Peschel, C.; Quirt, I.; Clark, J. I.; Wolchok, J. D.; Weber, J. S.; Tian, J.; Yellin, M. J.; Nichol, G. M.; Hoos, A.; Urba, W. J., Improved survival with ipilimumab in patients with metastatic melanoma. *N Engl J Med* **2010**, *363* (8), 711-23.
27. Topalian, S. L.; Hodi, F. S.; Brahmer, J. R.; Gettinger, S. N.; Smith, D. C.; McDermott, D. F.; Powderly, J. D.; Carvajal, R. D.; Sosman, J. A.; Atkins, M. B.; Leming, P. D.; Spigel, D. R.; Antonia, S. J.; Horn, L.; Drake, C. G.; Pardoll, D. M.; Chen, L.; Sharfman, W. H.; Anders, R. A.; Taube, J. M.; McMiller, T. L.; Xu, H.; Korman, A. J.; Jure-Kunkel, M.; Agrawal, S.; McDonald, D.; Kollia, G. D.; Gupta, A.; Wigginton, J. M.; Sznol, M., Safety, activity, and immune correlates of anti-PD-1 antibody in cancer. *N Engl J Med* **2012**, *366* (26), 2443-54.
28. Tchekmedyian, N.; Gray, J. E.; Creelan, B. C.; Chiappori, A. A.; Beg, A. A.; Soliman, H.; Perez, B. A.; Antonia, S. J., Propelling Immunotherapy Combinations Into the Clinic. *Oncology (Williston Park)* **2015**, *29* (12); Choudhury, N.; Nakamura, Y., The importance of

REFERENCES

- immunopharmacogenomics in cancer treatment: Patient Selection and Monitoring for Immune Checkpoint Antibodies. *Cancer Sci* **2015**.
29. Ishida, Y.; Agata, Y.; Shibahara, K.; Honjo, T., Induced expression of PD-1, a novel member of the immunoglobulin gene superfamily, upon programmed cell death. *Embo j* **1992**, *11* (11), 3887-95.
30. Kinter, A. L.; Godbout, E. J.; McNally, J. P.; Sereti, I.; Roby, G. A.; O'Shea, M. A.; Fauci, A. S., The common gamma-chain cytokines IL-2, IL-7, IL-15, and IL-21 induce the expression of programmed death-1 and its ligands. *J Immunol* **2008**, *181* (10), 6738-46.
31. Agata, Y.; Kawasaki, A.; Nishimura, H.; Ishida, Y.; Tsubata, T.; Yagita, H.; Honjo, T., Expression of the PD-1 antigen on the surface of stimulated mouse T and B lymphocytes. *Int Immunol* **1996**, *8* (5), 765-72.
32. Freeman, G. J.; Long, A. J.; Iwai, Y.; Bourque, K.; Chernova, T.; Nishimura, H.; Fitz, L. J.; Malenkovich, N.; Okazaki, T.; Byrne, M. C.; Horton, H. F.; Fouser, L.; Carter, L.; Ling, V.; Bowman, M. R.; Carreno, B. M.; Collins, M.; Wood, C. R.; Honjo, T., Engagement of the PD-1 immunoinhibitory receptor by a novel B7 family member leads to negative regulation of lymphocyte activation. *J Exp Med* **2000**, *192* (7), 1027-34.
33. Raimondi, G.; Shufesky, W. J.; Tokita, D.; Morelli, A. E.; Thomson, A. W., Regulated compartmentalization of programmed cell death-1 discriminates CD4+CD25+ resting regulatory T cells from activated T cells. *J Immunol* **2006**, *176* (5), 2808-16.
34. Dong, Q.; Siminovitch, K. A.; Fialkow, L.; Fukushima, T.; Downey, G. P., Negative regulation of myeloid cell proliferation and function by the SH2 domain-containing tyrosine phosphatase-1. *J Immunol* **1999**, *162* (6), 3220-30.
35. Tamura, H.; Dong, H.; Zhu, G.; Sica, G. L.; Flies, D. B.; Tamada, K.; Chen, L., B7-H1 costimulation preferentially enhances CD28-independent T-helper cell function. *Blood* **2001**, *97* (6), 1809-16.
36. Tseng, S. Y.; Otsuji, M.; Gorski, K.; Huang, X.; Slansky, J. E.; Pai, S. I.; Shalabi, A.; Shin, T.; Pardoll, D. M.; Tsuchiya, H., B7-DC, a new dendritic cell molecule with potent costimulatory properties for T cells. *J Exp Med* **2001**, *193* (7), 839-46.
37. Blank, C.; Kuball, J.; Voelkl, S.; Wiendl, H.; Becker, B.; Walter, B.; Majdic, O.; Gajewski, T. F.; Theobald, M.; Andreesen, R.; Mackensen, A., Blockade of PD-L1 (B7-H1) augments human tumor-specific T cell responses in vitro. *Int J Cancer* **2006**, *119* (2), 317-27; Blank, C.; Gajewski, T. F.; Mackensen, A., Interaction of PD-L1 on tumor cells with PD-1 on tumor-specific T cells as a mechanism of immune evasion: implications for tumor immunotherapy. *Cancer Immunol Immunother* **2005**, *54* (4), 307-14.
38. Butte, M. J.; Keir, M. E.; Phamduy, T. B.; Sharpe, A. H.; Freeman, G. J., Programmed death-1 ligand 1 interacts specifically with the B7-1 costimulatory molecule to inhibit T cell responses. *Immunity* **2007**, *27* (1), 111-22.
39. Butte, M. J.; Pena-Cruz, V.; Kim, M. J.; Freeman, G. J.; Sharpe, A. H., Interaction of human PD-L1 and B7-1. *Mol Immunol* **2008**, *45* (13), 3567-72.
40. Park, J. J.; Omiya, R.; Matsumura, Y.; Sakoda, Y.; Kuramasu, A.; Augustine, M. M.; Yao, S.; Tsushima, F.; Narazaki, H.; Anand, S.; Liu, Y.; Strome, S. E.; Chen, L.; Tamada, K., B7-H1/CD80 interaction is required for the induction and maintenance of peripheral T-cell tolerance. *Blood* **2010**, *116* (8), 1291-8.
41. Maenhout, S. K.; Van Lint, S.; Emeagi, P. U.; Thielemans, K.; Aerts, J. L., Enhanced suppressive capacity of tumor-infiltrating myeloid-derived suppressor cells compared with their peripheral counterparts. *Int J Cancer* **2014**, *134* (5), 1077-90.
42. J. Pen, J. A., Thérèse Liechtenstein, David Escors and Karine Breckpot, Immunology and Microbiology. In *Immune Response Activation*, May 29 2014.
43. Wang, L.; Pino-Lagos, K.; de Vries, V. C.; Guleria, I.; Sayegh, M. H.; Noelle, R. J., Programmed death 1 ligand signaling regulates the generation of adaptive Foxp3+CD4+ regulatory T cells. *Proc Natl Acad Sci U S A* **2008**, *105* (27), 9331-6.
44. Francisco, L. M.; Salinas, V. H.; Brown, K. E.; Vanguri, V. K.; Freeman, G. J.; Kuchroo, V. K.; Sharpe, A. H., PD-L1 regulates the development, maintenance, and function of induced regulatory T cells. *J Exp Med* **2009**, *206* (13), 3015-29.

REFERENCES

45. Fife, B. T.; Pauken, K. E.; Eagar, T. N.; Obu, T.; Wu, J.; Tang, Q.; Azuma, M.; Krummel, M. F.; Bluestone, J. A., Interactions between PD-1 and PD-L1 promote tolerance by blocking the TCR-induced stop signal. *Nat Immunol* **2009**, *10* (11), 1185-92.
46. Karwacz, K.; Arce, F.; Bricogne, C.; Kochan, G.; Escors, D., PD-L1 co-stimulation, ligand-induced TCR down-modulation and anti-tumor immunotherapy. *Oncoimmunology* **2012**, *1* (1), 86-88.
47. Karwacz, K.; Bricogne, C.; MacDonald, D.; Arce, F.; Bennett, C. L.; Collins, M.; Escors, D., PD-L1 co-stimulation contributes to ligand-induced T cell receptor down-modulation on CD8+ T cells. *EMBO Mol Med* **2011**, *3* (10), 581-92.
48. Liechtenstein, T.; Dufait, I.; Bricogne, C.; Lanna, A.; Pen, J.; Breckpot, K.; Escors, D., PD-L1/PD-1 Co-Stimulation, a Brake for T cell Activation and a T cell Differentiation Signal. *J Clin Cell Immunol* **2012**, *S12*.
49. Pen, J. J.; Keersmaecker, B. D.; Heirman, C.; Corthals, J.; Liechtenstein, T.; Escors, D.; Thielemans, K.; Breckpot, K., Interference with PD-L1/PD-1 co-stimulation during antigen presentation enhances the multifunctionality of antigen-specific T cells. *Gene Ther* **2014**.
50. Casey, S. C.; Tong, L.; Li, Y.; Do, R.; Walz, S.; Fitzgerald, K. N.; Gouw, A. M.; Baylot, V.; Gutgemann, I.; Eilers, M.; Felsher, D. W., MYC regulates the antitumor immune response through CD47 and PD-L1. *Science* **2016**.
51. Hugo, W.; Zaretsky, J. M.; Sun, L.; Song, C.; Moreno, B. H.; Hu-Lieskovan, S.; Berent-Maoz, B.; Pang, J.; Chmielowski, B.; Cherry, G.; Seja, E.; Lomeli, S.; Kong, X.; Kelley, M. C.; Sosman, J. A.; Johnson, D. B.; Ribas, A.; Lo, R. S., Genomic and Transcriptomic Features of Response to Anti-PD-1 Therapy in Metastatic Melanoma. *Cell* **2016**, *165* (1), 35-44.
52. Taube, J. M.; Anders, R. A.; Young, G. D.; Xu, H.; Sharma, R.; McMiller, T. L.; Chen, S.; Klein, A. P.; Pardoll, D. M.; Topalian, S. L.; Chen, L., Colocalization of inflammatory response with B7-h1 expression in human melanocytic lesions supports an adaptive resistance mechanism of immune escape. *Sci Transl Med* **2012**, *4* (127), 127ra37.
53. Azuma, T.; Yao, S.; Zhu, G.; Flies, A. S.; Flies, S. J.; Chen, L., B7-H1 is a ubiquitous antiapoptotic receptor on cancer cells. *Blood* **2008**, *111* (7), 3635-43.
54. Hirano, F.; Kaneko, K.; Tamura, H.; Dong, H.; Wang, S.; Ichikawa, M.; Rietz, C.; Flies, D. B.; Lau, J. S.; Zhu, G.; Tamada, K.; Chen, L., Blockade of B7-H1 and PD-1 by monoclonal antibodies potentiates cancer therapeutic immunity. *Cancer Res* **2005**, *65* (3), 1089-96.
55. Iwai, Y.; Ishida, M.; Tanaka, Y.; Okazaki, T.; Honjo, T.; Minato, N., Involvement of PD-L1 on tumor cells in the escape from host immune system and tumor immunotherapy by PD-L1 blockade. *Proc Natl Acad Sci U S A* **2002**, *99* (19), 12293-7.
56. Dong, H.; Strome, S. E.; Salomao, D. R.; Tamura, H.; Hirano, F.; Flies, D. B.; Roche, P. C.; Lu, J.; Zhu, G.; Tamada, K.; Lennon, V. A.; Celis, E.; Chen, L., Tumor-associated B7-H1 promotes T-cell apoptosis: a potential mechanism of immune evasion. *Nat Med* **2002**, *8* (8), 793-800.
57. Hamanishi, J.; Mandai, M.; Iwasaki, M.; Okazaki, T.; Tanaka, Y.; Yamaguchi, K.; Higuchi, T.; Yagi, H.; Takakura, K.; Minato, N.; Honjo, T.; Fujii, S., Programmed cell death 1 ligand 1 and tumor-infiltrating CD8+ T lymphocytes are prognostic factors of human ovarian cancer. *Proc Natl Acad Sci U S A* **2007**, *104* (9), 3360-5.
58. Maine, C. J.; Aziz, N. H.; Chatterjee, J.; Hayford, C.; Brewig, N.; Whilding, L.; George, A. J.; Ghaem-Maghami, S., Programmed death ligand-1 over-expression correlates with malignancy and contributes to immune regulation in ovarian cancer. *Cancer Immunol Immunother* **2014**, *63* (3), 215-24.
59. Thompson, R. H.; Gillett, M. D.; Cheville, J. C.; Lohse, C. M.; Dong, H.; Webster, W. S.; Chen, L.; Zincke, H.; Blute, M. L.; Leibovich, B. C.; Kwon, E. D., Costimulatory molecule B7-H1 in primary and metastatic clear cell renal cell carcinoma. *Cancer* **2005**, *104* (10), 2084-91.
60. Nomi, T.; Sho, M.; Akahori, T.; Hamada, K.; Kubo, A.; Kanehiro, H.; Nakamura, S.; Enomoto, K.; Yagita, H.; Azuma, M.; Nakajima, Y., Clinical significance and therapeutic

REFERENCES

- potential of the programmed death-1 ligand/programmed death-1 pathway in human pancreatic cancer. *Clin Cancer Res* **2007**, *13* (7), 2151-7.
61. Gao, Q.; Wang, X. Y.; Qiu, S. J.; Yamato, I.; Sho, M.; Nakajima, Y.; Zhou, J.; Li, B. Z.; Shi, Y. H.; Xiao, Y. S.; Xu, Y.; Fan, J., Overexpression of PD-L1 significantly associates with tumor aggressiveness and postoperative recurrence in human hepatocellular carcinoma. *Clin Cancer Res* **2009**, *15* (3), 971-9.
62. Ghebeh, H.; Mohammed, S.; Al-Omair, A.; Qattan, A.; Lehe, C.; Al-Qudaihi, G.; Elkum, N.; Alshabanah, M.; Bin Amer, S.; Tulbah, A.; Ajarim, D.; Al-Tweigeri, T.; Dermime, S., The B7-H1 (PD-L1) T lymphocyte-inhibitory molecule is expressed in breast cancer patients with infiltrating ductal carcinoma: correlation with important high-risk prognostic factors. *Neoplasia* **2006**, *8* (3), 190-8.
63. Muenst, S.; Schaeferli, A. R.; Gao, F.; Daster, S.; Trella, E.; Drosner, R. A.; Muraro, M. G.; Zajac, P.; Zanetti, R.; Gillanders, W. E.; Weber, W. P.; Soysal, S. D., Expression of programmed death ligand 1 (PD-L1) is associated with poor prognosis in human breast cancer. *Breast Cancer Res Treat* **2014**, *146* (1), 15-24.
64. Hamid, O.; Robert, C.; Daud, A.; Hodi, F. S.; Hwu, W. J.; Kefford, R.; Wolchok, J. D.; Hersey, P.; Joseph, R. W.; Weber, J. S.; Dronca, R.; Gangadhar, T. C.; Patnaik, A.; Zarour, H.; Joshua, A. M.; Gergich, K.; Ellassaiss-Schaap, J.; Algazi, A.; Mateus, C.; Boasberg, P.; Tume, P. C.; Chmielowski, B.; Ebbinghaus, S. W.; Li, X. N.; Kang, S. P.; Ribas, A., Safety and tumor responses with lambrolizumab (anti-PD-1) in melanoma. *N Engl J Med* **2013**, *369* (2), 134-44; Topalian, S. L.; Sznol, M.; McDermott, D. F.; Kluger, H. M.; Carvajal, R. D.; Sharfman, W. H.; Brahmer, J. R.; Lawrence, D. P.; Atkins, M. B.; Powderly, J. D.; Leming, P. D.; Lipson, E. J.; Puzanov, I.; Smith, D. C.; Taube, J. M.; Wigginton, J. M.; Kollia, G. D.; Gupta, A.; Pardoll, D. M.; Sosman, J. A.; Hodi, F. S., Survival, durable tumor remission, and long-term safety in patients with advanced melanoma receiving nivolumab. *J Clin Oncol* **2014**, *32* (10), 1020-30.
65. Postow, M. A.; Callahan, M. K.; Wolchok, J. D., Immune Checkpoint Blockade in Cancer Therapy. *J Clin Oncol* **2015**, *33* (17), 1974-82.
66. Robert, C.; Ribas, A.; Wolchok, J. D.; Hodi, F. S.; Hamid, O.; Kefford, R.; Weber, J. S.; Joshua, A. M.; Hwu, W. J.; Gangadhar, T. C.; Patnaik, A.; Dronca, R.; Zarour, H.; Joseph, R. W.; Boasberg, P.; Chmielowski, B.; Mateus, C.; Postow, M. A.; Gergich, K.; Ellassaiss-Schaap, J.; Li, X. N.; Iannone, R.; Ebbinghaus, S. W.; Kang, S. P.; Daud, A., Anti-programmed-death-receptor-1 treatment with pembrolizumab in ipilimumab-refractory advanced melanoma: a randomised dose-comparison cohort of a phase 1 trial. *Lancet* **2014**, *384* (9948), 1109-17.
67. Berger, R.; Rotem-Yehudar, R.; Slama, G.; Landes, S.; Kneller, A.; Leiba, M.; Koren-Michowitz, M.; Shimoni, A.; Nagler, A., Phase I safety and pharmacokinetic study of CT-011, a humanized antibody interacting with PD-1, in patients with advanced hematologic malignancies. *Clin Cancer Res* **2008**, *14* (10), 3044-51; Armand, P.; Nagler, A.; Weller, E. A.; Devine, S. M.; Avigan, D. E.; Chen, Y. B.; Kaminski, M. S.; Holland, H. K.; Winter, J. N.; Mason, J. R.; Fay, J. W.; Rizzieri, D. A.; Hosing, C. M.; Ball, E. D.; Uberti, J. P.; Lazarus, H. M.; Mapara, M. Y.; Gregory, S. A.; Timmerman, J. M.; Andorsky, D.; Or, R.; Waller, E. K.; Rotem-Yehudar, R.; Gordon, L. I., Disabling immune tolerance by programmed death-1 blockade with pidilizumab after autologous hematopoietic stem-cell transplantation for diffuse large B-cell lymphoma: results of an international phase II trial. *J Clin Oncol* **2013**, *31* (33), 4199-206.
68. Zou, W.; Wolchok, J. D.; Chen, L., PD-L1 (B7-H1) and PD-1 pathway blockade for cancer therapy: Mechanisms, response biomarkers, and combinations. *Sci Transl Med* **2016**, *8* (328), 328rv4.
69. Liu, X.; Gao, J. X.; Wen, J.; Yin, L.; Li, O.; Zuo, T.; Gajewski, T. F.; Fu, Y. X.; Zheng, P.; Liu, Y., B7DC/PDL2 promotes tumor immunity by a PD-1-independent mechanism. *J Exp Med* **2003**, *197* (12), 1721-30; Shin, T.; Kennedy, G.; Gorski, K.; Tsuchiya, H.; Koseki, H.; Azuma, M.; Yagita, H.; Chen, L.; Powell, J.; Pardoll, D.; Housseau, F., Cooperative B7-1/2 (CD80/CD86) and B7-DC costimulation of CD4+ T cells independent of the PD-1 receptor. *J Exp Med* **2003**, *198* (1), 31-8; Shin, T.; Yoshimura, K.; Crafton, E. B.; Tsuchiya, H.;

REFERENCES

- Housseau, F.; Koseki, H.; Schulick, R. D.; Chen, L.; Pardoll, D. M., In vivo costimulatory role of B7-DC in tuning T helper cell 1 and cytotoxic T lymphocyte responses. *J Exp Med* **2005**, *201* (10), 1531-41.
70. Brahmer, J. R.; Tykodi, S. S.; Chow, L. Q.; Hwu, W. J.; Topalian, S. L.; Hwu, P.; Drake, C. G.; Camacho, L. H.; Kauh, J.; Odunsi, K.; Pitot, H. C.; Hamid, O.; Bhatia, S.; Martins, R.; Eaton, K.; Chen, S.; Salay, T. M.; Alaparthi, S.; Grosso, J. F.; Korman, A. J.; Parker, S. M.; Agrawal, S.; Goldberg, S. M.; Pardoll, D. M.; Gupta, A.; Wigginton, J. M., Safety and activity of anti-PD-L1 antibody in patients with advanced cancer. *N Engl J Med* **2012**, *366* (26), 2455-65.
71. Homet Moreno, B.; Ribas, A., Anti-programmed cell death protein-1/ligand-1 therapy in different cancers. *Br J Cancer* **2015**, *112* (9), 1421-7.
72. Herbst, R. S.; Soria, J. C.; Kowanetz, M.; Fine, G. D.; Hamid, O.; Gordon, M. S.; Sosman, J. A.; McDermott, D. F.; Powderly, J. D.; Gettinger, S. N.; Kohrt, H. E.; Horn, L.; Lawrence, D. P.; Rost, S.; Leabman, M.; Xiao, Y.; Mokatrini, A.; Koeppen, H.; Hegde, P. S.; Mellman, I.; Chen, D. S.; Hodi, F. S., Predictive correlates of response to the anti-PD-L1 antibody MPDL3280A in cancer patients. *Nature* **2014**, *515* (7528), 563-7.
73. Weber, J. S.; D'Angelo, S. P.; Minor, D.; Hodi, F. S.; Gutzmer, R.; Neyns, B.; Hoeller, C.; Khushalani, N. I.; Miller, W. H., Jr.; Lao, C. D.; Linette, G. P.; Thomas, L.; Lorigan, P.; Grossmann, K. F.; Hassel, J. C.; Maio, M.; Sznol, M.; Ascierto, P. A.; Mohr, P.; Chmielowski, B.; Bryce, A.; Svane, I. M.; Grob, J. J.; Krackhardt, A. M.; Horak, C.; Lambert, A.; Yang, A. S.; Larkin, J., Nivolumab versus chemotherapy in patients with advanced melanoma who progressed after anti-CTLA-4 treatment (CheckMate 037): a randomised, controlled, open-label, phase 3 trial. *Lancet Oncol* **2015**, *16* (4), 375-84.
74. Boyerinas, B.; Jochems, C.; Fantini, M.; Heery, C. R.; Gulley, J. L.; Tsang, K. Y.; Schlom, J., Antibody-Dependent Cellular Cytotoxicity Activity of a Novel Anti-PD-L1 Antibody Avelumab (MSB0010718C) on Human Tumor Cells. *Cancer Immunol Res* **2015**, *3* (10), 1148-57.
75. Ahmadzadeh, M.; Johnson, L. A.; Heemskerk, B.; Wunderlich, J. R.; Dudley, M. E.; White, D. E.; Rosenberg, S. A., Tumor antigen-specific CD8 T cells infiltrating the tumor express high levels of PD-1 and are functionally impaired. *Blood* **2009**, *114* (8), 1537-44; Chapon, M.; Randriamampita, C.; Maubec, E.; Badoual, C.; Fouquet, S.; Wang, S. F.; Marinho, E.; Farhi, D.; Garcette, M.; Jacobelli, S.; Rouquette, A.; Carlotti, A.; Girod, A.; Prevost-Blondel, A.; Trautmann, A.; Avril, M. F.; Bercovici, N., Progressive upregulation of PD-1 in primary and metastatic melanomas associated with blunted TCR signaling in infiltrating T lymphocytes. *J Invest Dermatol* **2011**, *131* (6), 1300-7; French, J. D.; Kotnis, G. R.; Said, S.; Raeburn, C. D.; McIntyre, R. C., Jr.; Kloppner, J. P.; Haugen, B. R., Programmed death-1+ T cells and regulatory T cells are enriched in tumor-involved lymph nodes and associated with aggressive features in papillary thyroid cancer. *J Clin Endocrinol Metab* **2012**, *97* (6), E934-43.
76. Chatterjee, S.; Lesniak, W. G.; Gabrielson, M.; Lisok, A.; Wharram, B.; Sysa-Shah, P.; Azad, B. B.; Pomper, M. G.; Nimmagadda, S., A humanized antibody for imaging immune checkpoint ligand PD-L1 expression in tumors. *Oncotarget* **2016**.
77. Teng, M. W.; Ngiow, S. F.; Ribas, A.; Smyth, M. J., Classifying Cancers Based on T-cell Infiltration and PD-L1. *Cancer Res* **2015**, *75* (11), 2139-45; Hill, J. A.; Feuerer, M.; Tash, K.; Haxhinasto, S.; Perez, J.; Melamed, R.; Mathis, D.; Benoist, C., Foxp3 transcription-factor-dependent and -independent regulation of the regulatory T cell transcriptional signature. *Immunity* **2007**, *27* (5), 786-800.
78. Heskamp, S.; Hobo, W.; Molkenboer-Kuennen, J. D.; Olive, D.; Oyen, W. J.; Dolstra, H.; Boerman, O. C., Noninvasive Imaging of Tumor PD-L1 Expression Using Radiolabeled Anti-PD-L1 Antibodies. *Cancer Res* **2015**, *75* (14), 2928-36.
79. Josefsson, A.; Nedrow, J. R.; Park, S.; Banerjee, S. R.; Rittenbach, A.; Jammes, F.; Tsui, B.; Sgouros, G., Imaging, Biodistribution, and Dosimetry of Radionuclide-Labeled PD-L1 Antibody in an Immunocompetent Mouse Model of Breast Cancer. *Cancer Res* **2016**, *76* (2), 472-9; Maute, R. L.; Gordon, S. R.; Mayer, A. T.; McCracken, M. N.; Natarajan, A.; Ring, N. G.; Kimura, R.; Tsai, J. M.; Manglik, A.; Kruse, A. C.; Gambhir, S. S.; Weissman, I. L.;

REFERENCES

- Ring, A. M., Engineering high-affinity PD-1 variants for optimized immunotherapy and immuno-PET imaging. *Proc Natl Acad Sci U S A* **2015**, *112* (47), E6506-14.
80. Natarajan, A.; Mayer, A. T.; Xu, L.; Reeves, R. E.; Gano, J.; Gambhir, S. S., Novel Radiotracer for ImmunoPET Imaging of PD-1 Checkpoint Expression on Tumor Infiltrating Lymphocytes. *Bioconjug Chem* **2015**, *26* (10), 2062-9.
81. Fransen, M. F.; van der Sluis, T. C.; Ossendorp, F.; Arens, R.; Melief, C. J., Controlled local delivery of CTLA-4 blocking antibody induces CD8+ T-cell-dependent tumor eradication and decreases risk of toxic side effects. In *Clin Cancer Res*, 2013 Aacr.: United States, 2013; Vol. 19, pp 5381-9.
82. Chames, P.; Van Regenmortel, M.; Weiss, E.; Baty, D., Therapeutic antibodies: successes, limitations and hopes for the future. *Br J Pharmacol* **2009**, *157* (2), 220-33.
83. Pardoll, D. M., The blockade of immune checkpoints in cancer immunotherapy. *Nat Rev Cancer* **2012**, *12* (4), 252-64; Andrews, A., Treating with Checkpoint Inhibitors-Figure \$1 Million per Patient. *Am Health Drug Benefits* **2015**, *8* (Spec Issue), 9.
84. Chakravarty, R.; Goel, S.; Cai, W., Nanobody: the "magic bullet" for molecular imaging? *Theranostics* **2014**, *4* (4), 386-98.
85. Vaneycken, I.; Devoogdt, N.; Van Gassen, N.; Vincke, C.; Xavier, C.; Wernery, U.; Muyldermans, S.; Lahoutte, T.; Caveliers, V., Preclinical screening of anti-HER2 nanobodies for molecular imaging of breast cancer. *Faseb j* **2011**, *25* (7), 2433-46.
86. Pruszyński, M.; Koumariyanou, E.; Vaidyanathan, G.; Revets, H.; Devoogdt, N.; Lahoutte, T.; Zalutsky, M. R., Targeting breast carcinoma with radioiodinated anti-HER2 Nanobody. *Nucl Med Biol* **2013**, *40* (1), 52-9; D'Huyvetter, M.; Aerts, A.; Xavier, C.; Vaneycken, I.; Devoogdt, N.; Gijs, M.; Impens, N.; Baatout, S.; Ponsard, B.; Muyldermans, S.; Caveliers, V.; Lahoutte, T., Development of 177Lu-nanobodies for radioimmunotherapy of HER2-positive breast cancer: evaluation of different bifunctional chelators. *Contrast Media Mol Imaging* **2012**, *7* (2), 254-64.
87. Gaikam, L. O.; Caveliers, V.; Devoogdt, N.; Vanhove, C.; Xavier, C.; Boerman, O.; Muyldermans, S.; Bossuyt, A.; Lahoutte, T., Localization, mechanism and reduction of renal retention of technetium-99m labeled epidermal growth factor receptor-specific nanobody in mice. *Contrast Media Mol Imaging* **2011**, *6* (2), 85-92.
88. Vaneycken, I.; Govaert, J.; Vincke, C.; Caveliers, V.; Lahoutte, T.; De Baetselier, P.; Raes, G.; Bossuyt, A.; Muyldermans, S.; Devoogdt, N., In vitro analysis and in vivo tumor targeting of a humanized, grafted nanobody in mice using pinhole SPECT/micro-CT. *J Nucl Med* **2010**, *51* (7), 1099-106.
89. Movahedi, K.; Schoonoghe, S.; Laoui, D.; Houbracken, I.; Waelput, W.; Breckpot, K.; Bouwens, L.; Lahoutte, T.; De Baetselier, P.; Raes, G.; Devoogdt, N.; Van Ginderachter, J. A., Nanobody-based targeting of the macrophage mannose receptor for effective in vivo imaging of tumor-associated macrophages. *Cancer Res* **2012**, *72* (16), 4165-77.
90. Breckpot, K.; Dullaers, M.; Bonehill, A.; van Meirvenne, S.; Heirman, C.; de Greef, C.; van der Bruggen, P.; Thielemans, K., Lentivirally transduced dendritic cells as a tool for cancer immunotherapy. *J Gene Med* **2003**, *5* (8), 654-67.
91. Liechtenstein, T.; Perez-Janices, N.; Blanco-Luquin, I.; Goyvaerts, C.; Schwarze, J.; Dufait, I.; Lanna, A.; Ridder, M.; Guerrero-Setas, D.; Breckpot, K.; Escors, D., Anti-melanoma vaccines engineered to simultaneously modulate cytokine priming and silence PD-L1 characterized using myeloid-derived suppressor cells as a readout of therapeutic efficacy. *Oncoimmunology* **2014**, *3* (7), e945378.
92. Goyvaerts, C.; De Groeve, K.; Dingemans, J.; Van Lint, S.; Robays, L.; Heirman, C.; Reiser, J.; Zhang, X. Y.; Thielemans, K.; De Baetselier, P.; Raes, G.; Breckpot, K., Development of the Nanobody display technology to target lentiviral vectors to antigen-presenting cells. *Gene Ther* **2012**, *19* (12), 1133-40.
93. Rosenberg, S. A.; Yang, J. C.; Sherry, R. M.; Kammula, U. S.; Hughes, M. S.; Phan, G. Q.; Citrin, D. E.; Restifo, N. P.; Robbins, P. F.; Wunderlich, J. R.; Morton, K. E.; Laurencot, C. M.; Steinberg, S. M.; White, D. E.; Dudley, M. E., Durable complete responses in heavily pretreated patients with metastatic melanoma using T-cell transfer immunotherapy. *Clin Cancer Res* **2011**, *17* (13), 4550-7.

REFERENCES

94. Wilgenhof, S.; Van Nuffel, A. M.; Corthals, J.; Heirman, C.; Tuyaerts, S.; Benteyn, D.; De Coninck, A.; Van Riet, I.; Verfaillie, G.; Vandeloo, J.; Bonehill, A.; Thielemans, K.; Neyns, B., Therapeutic vaccination with an autologous mRNA electroporated dendritic cell vaccine in patients with advanced melanoma. *J Immunother* **2011**, *34* (5), 448-56.
95. Devoogdt, N.; Xavier, C.; Hernot, S.; Vaneycken, I.; D'Huyvetter, M.; De Vos, J.; Massa, S.; De Baetselier, P.; Caveliere, V.; Lahoutte, T., Molecular imaging using Nanobodies: a case study. *Methods Mol Biol* **2012**, *911*, 559-67.
96. Tijink, B. M.; Laeremans, T.; Budde, M.; Stigter-van Walsum, M.; Dreier, T.; de Haard, H. J.; Leemans, C. R.; van Dongen, G. A., Improved tumor targeting of anti-epidermal growth factor receptor Nanobodies through albumin binding: taking advantage of modular Nanobody technology. *Mol Cancer Ther* **2008**, *7* (8), 2288-97.
97. Lin, Y. M.; Sung, W. W.; Hsieh, M. J.; Tsai, S. C.; Lai, H. W.; Yang, S. M.; Shen, K. H.; Chen, M. K.; Lee, H.; Yeh, K. T.; Chen, C. J., High PD-L1 Expression Correlates with Metastasis and Poor Prognosis in Oral Squamous Cell Carcinoma. *PLoS One* **2015**, *10* (11), e0142656.
98. Taube, J. M.; Klein, A.; Brahmer, J. R.; Xu, H.; Pan, X.; Kim, J. H.; Chen, L.; Pardoll, D. M.; Topalian, S. L.; Anders, R. A., Association of PD-1, PD-1 ligands, and other features of the tumor immune microenvironment with response to anti-PD-1 therapy. *Clin Cancer Res* **2014**, *20* (19), 5064-74.
99. Travis, J., Making the cut. In *Science*, United States, 2015; Vol. 350, pp 1456-7.